

2008

Multipole Methods in Potential Theory

Steve W. Campbell
Western University

Follow this and additional works at: <https://ir.lib.uwo.ca/digitizedtheses>

Recommended Citation

Campbell, Steve W., "Multipole Methods in Potential Theory" (2008). *Digitized Theses*. 4362.
<https://ir.lib.uwo.ca/digitizedtheses/4362>

This Thesis is brought to you for free and open access by the Digitized Special Collections at Scholarship@Western. It has been accepted for inclusion in Digitized Theses by an authorized administrator of Scholarship@Western. For more information, please contact wlsadmin@uwo.ca.

Multipole Methods in Potential Theory
(Thesis Format: Monograph)

by

Steve W. Campbell

Graduate Program in Applied Mathematics

A thesis submitted in partial fulfillment
of the requirements for the degree of
Master of Science

/

School of Graduate and Postdoctoral Studies
The University of Western Ontario
London, Ontario, Canada

© Steve W. Campbell, 2008

THE UNIVERSITY OF WESTERN ONTARIO
SCHOOL OF GRADUATE AND POSTDOCTORAL STUDIES

CERTIFICATE OF EXAMINATION

Advisor:

Examining Board:

Dr. David J. Jeffrey

Dr. V. Miransky

Dr. C. Essex

Dr. M. Floryan

The thesis by
Steve W. Campbell

entitled:
Multipole Methods in Potential Theory

is accepted in partial fulfillment of the
requirements for the degree of
Master of Science

October 7, 2008
Date

Chair of Examining Board
Dr. H. Rasmussen

Abstract

This thesis calculates the potential resulting from a sphere placed inside of a cylinder of infinite length with a uniform field imposed at infinity. We start with a general discussion on axial and general multipoles in physics. We discuss how a potential function can be found by solving the Laplace equation in spherical or cylindrical coordinates and how this technique is equivalent to finding the multipoles. We calculate the potential resulting from a sphere placed inside of a cylindrical tube. We do this by transferring multipoles expressed in cylindrical coordinates to spherical coordinates. The strengths of the multipoles are obtained as power series in the ratio of the radii of the sphere and the cylinder. The dipole strength of the sphere gives the increase of the potential drop along the cylinder. The presence of this sphere is electrically equivalent to increasing the length of the cylindrical tube. The new feature of this solution is the possibility of obtaining the analytic form of the singular behaviour of the solution.

Keywords: Multipoles, Laplace equation, Electromagnetics, Electrostatics, Fluid mechanics, Asymptotics

Acknowledgements

I would like to thank my girlfriend Lindsay Gee for her continued love and support. I would also like to thank my supervisor David Jeffrey. His guidance, encouragement, and seemingly unlimited patience made this thesis possible. I would also like to thank Vladimir Miransky and Christopher Essex for their outstanding teaching and for igniting my interest in applied mathematics. Finally, I would like to thank Pat Malone and Audrey Kager for welcoming me into the department.

Contents

Certificate of Examination	ii
Abstract	iii
Acknowledgements	iv
List of Tables	vii
List of Figures	viii
1 Introduction	1
2 General Information on Multipoles in Physics	4
2.1 Axial Multipoles	4
2.1.1 Potential due to a Point Charge	4
2.1.2 Potential due to a Line of Charge	7
2.1.3 The Dipole Term	9
2.1.4 The Quadrupole Term	12
2.1.5 Higher Order Terms	12
2.2 General Multipoles	14
2.3 Solving Electrostatic Problems with Multipoles	17
2.3.1 Method of Images for a Grounded Sphere	17
2.3.2 Replacing an Image Charge with a Multipole	19
2.4 Solution of the Laplace Equation in Spherical Coordinates	20

2.5	Solution of the Laplace Equation in Cylindrical Coordinates	23
3	The Potential around a Sphere inside a Cylinder	27
3.1	Solution of Sphere Problem	28
3.2	Numerical Calculation of B_{mn}	39
3.3	Numerical Calculation of K_{np} Coefficients	45
3.4	Expression for Potential Drop	47
3.5	Asymptotic Behaviour	48
3.6	Expansion of $\left(\frac{-1}{p}\right)$	52
3.7	Conclusions	56
	Bibliography	57
	Vitae	60

List of Tables

3.1	The computed value of $K_{(1)(81)}$ and the computation time for various values of <i>ChangeoverParameter</i> . The computation time appears to be erratic because the method of measurement is not sufficiently accurate.	47
3.2	The increase in resistance of a solid conducting cylinder due to the presence of a spherical bubble, or the effective increase in the length of the cylinder	54

List of Figures

2.1	Graph showing the location of an arbitrary point P in relation to a point charge located on the z -axis at $z = \zeta$	5
2.2	Graph showing the location of an arbitrary point P in relation to a line of charge that starts at the origin and ends at $z = l$	7
2.3	Graph showing the location of an arbitrary point P in relation to two point charges. One point charge has a charge of $-q$ and is located at the origin. The other point charge has a charge of $+q$ and is located on the z -axis at $z = l_0$	10
2.4	Graph showing the vectors that can be used to rewrite (2.14). \mathbf{p} is directed along the z -axis from the origin towards the positive point charge and has a magnitude of ql_0 . \mathbf{p}^0 is a unit vector directed from the origin towards the arbitrary point.	11
2.5	Graph showing the location of an arbitrary point P in relation to two dipoles. One dipole has a moment of $-p^{(1)}$ and is located at the origin. The other dipole has a moment of $+p^{(1)}$ and is located on the z -axis at $z = l_1$	13
2.6	Graph showing the location of an arbitrary point P in relation to two multipoles of order $n - 1$. One multipole has a moment of $-p^{(n-1)}$ and is located at the origin. The other multipole has a moment of $+p^{(n-1)}$ and is located on the z -axis at $z = l_n$	14

2.7	Graph showing the location of a point P that is arbitrarily located outside of the sphere. A differential element of charge dq is located arbitrarily inside the sphere. $\boldsymbol{\rho}$ is the vector from the origin to P . $\boldsymbol{\rho}_1 = \xi\mathbf{i} + \eta\mathbf{j} + \zeta\mathbf{k}$ is the vector from the origin to dq . $\boldsymbol{\rho}_2$ is the vector from dq to P	15
2.8	Graph showing a grounded sphere with a radius of a that is centered at the origin, a point charge with a magnitude of q that is located on the z -axis at $z = s$ where $a < s$, and a point P that is arbitrarily located outside of the sphere.	17
2.9	Graph showing a point charge with a magnitude of q that is located on the z -axis at $z = s$ where $a < s$, an image charge with a magnitude of $-q\frac{b}{a}$ that is located on the z -axis at $z = b = \frac{a^2}{s}$, and a point P that is arbitrarily located outside of the sphere.	19
2.10	Graph showing the relationship between spherical coordinates and rectangular coordinates.	21
2.11	Graph showing the relationship between cylindrical coordinates and rectangular coordinates.	24
3.1	The coordinate systems for the sphere inside the cylinder.	29
3.2	The domain for the double-summation $\sum_{m=1}^{\infty} \sum_{p=2n+2m-1}^{\infty} \dots$ in (3.14). The double-summation is reversed to $\sum_{p=2n+1}^{\infty} \sum_{m=1}^{\frac{p+1-2n}{2}}$ in (3.15).	37

3.3	The dependencies for many of the K_{np} coefficients. The dashed line follows the equation $p = 2n$. All of the coefficients that are on or below this line are 0 except for k_{10} which is 1. Above the dashed line, all of the coefficients have potentially non-zero values that are dependent on other K_{np} coefficients. The solid-lined arrows indicate these dependencies for some of the coefficients. For example, $K_{(2)(10)}$ is dependent on K_{27} , K_{35} , and K_{43} . The dependencies for many of the coefficients are omitted to make the figure less cluttered.	38
3.4	Graph showing three different integrands with respect to t . The top plot is the original integrand $\frac{t^{2(j-1)}}{I_1^2(t)}$ with $j = 2$. The middle plot is the original integrand with the first and second asymptotic expansion terms subtracted. The bottom plot is the original integrand with the first, second, third, and fourth asymptotic expansion terms subtracted.	42
3.5	Graph showing three different integrands with respect to t . The top plot is the original integrand $\frac{t^{2(j-1)}}{I_1^2(t)}$ with $j = 4$. The middle plot is the original integrand with the first and second asymptotic expansion terms subtracted. The bottom plot is the original integrand with the first, second, third, and fourth asymptotic expansion terms subtracted.	43
3.6	Graph showing three different integrands with respect to t . The top plot is the original integrand $\frac{t^{2(j-1)}}{I_1^2(t)}$ with $j = 12$. The middle plot is the original integrand with the first asymptotic expansion term subtracted. The bottom plot is the original integrand with the first and second asymptotic expansion terms subtracted.	44
3.7	A zoomed in view of the bottom portion of Figure 3.6.	44
3.8	The geometry that used to obtain the asymptotic approximation. It is supposed that the gap between the sphere and the cylinder is ϵ and the extent of the gap in the z direction is $\sqrt{\epsilon}$	49

3.9	Graph of $\frac{K_{1p}}{\frac{\pi}{2\sqrt{2}}(-1)^p \binom{-\frac{1}{2}}{p}}$ versus p . This expression approaches 1 as p approaches infinity.	51
3.10	Graph of $\frac{K_{1p} - \frac{\pi}{2\sqrt{2}}(-1)^p \binom{-\frac{1}{2}}{p^2}}{(-1)^p \binom{\frac{1}{2}}{p}}$ versus p . This expression approaches a constant value as p approaches infinity.	53
3.11	Graph of $\frac{K_{1p} - \frac{\pi}{2\sqrt{2}}(-1)^p \binom{-\frac{1}{2}}{p}}{2\sqrt{2}(-1)^p \binom{\frac{1}{2}}{p}}$ versus p . This expression approaches 1 as p approaches infinity.	54

Chapter 1

Introduction

From the point of view of modern theoretical physics, the Laplace equation is a classical equation that has been thoroughly studied. From the point of view of science and engineering, the Laplace equation requires further study. The properties of the equation itself are well understood. However, the detailed properties and implications of its solutions for technical applications require further study. Most engineering is based on classical physics.

This thesis examines one way to improve the efficiency of solving the Laplace equation and obtaining information about the properties of the solutions. These techniques are likely extensible to other classical equations such as the Helmholtz equation and the Stokes equation. The main feature of this technique is that the symbolic information is retained in an otherwise numerical solution.

In theoretical physics, many problems are solved using purely symbolic methods. These are usually simple problems such as a sphere falling slowly through an infinite fluid or flow past a two-dimensional airfoil. Purely symbolic methods are often unsuitable for realistic problems which tend to be more complicated. Happel and Brenner [1] used traditional symbolic methods of fluid mechanics to approximately calculate flow around a small sphere in a relatively large tube. However, their methods

are inaccurate if the sphere is large in relation to the diameter of the tube. Those who support purely numerical methods argue that symbolic methods are poorly suited to more complicated flow problems such as this one. As numerical methods become increasingly feasible, symbolic methods are becoming less and less prevalent in many areas of physics and engineering as they are typically used only in the initial set-up of problems.

We use a symbolic-numeric approach to solve one class of physics problems. To describe this class of problems, we use the problem of a non-conducting sphere that is placed in the center of an infinitely long conducting cylinder. We start with an expansion in eigenfunctions which is a traditional symbolic method in 19th century physics. The difficulty arises in computing the coefficients, so we do this numerically. However, the series converges very slowly, so we combine the numerical calculation of the coefficients with a symbolic analysis of the series to obtain a useful expression for the increase in the resistance of the wire that results from the placement of the sphere.

A crucial parameter in this problem is the ratio of the diameter of the sphere to the diameter of the cylinder. Purely symbolic methods become progressively less accurate as this ratio approaches 1. However, purely numerical methods do not retain symbolic information which is very useful. A numerical solution is valid for only a single ratio of diameters. The method described in this thesis overcomes the shortcomings of both a purely symbolic approach and a purely numerical approach. The ratio of diameters is present in the solution and the solution is valid for any ratio. The presence of this parameter in the solution allows for the analytical study of the singular behaviour that occurs as the parameter approaches 1.

It is important to note that, for this problem, the information that is required from the solution greatly influences the best method of solving the problem. The method presented in this thesis is well-suited for obtaining the increase in the resistance of the

Chapter 2

General Information on Multipoles in Physics

Multipoles offer a convenient way of understanding and deriving solutions of the Laplace equation and other equations such as the linearized equations of fluid mechanics. This chapter introduces the basic theory.

2.1 Axial Multipoles

This section discusses multipole expansions of charge distributions located on the z -axis only.

2.1.1 Potential due to a Point Charge

Figure 2.1 shows an arbitrary point P and a point charge of size q located on the z -axis at $z = \zeta$. Let ρ be the distance between P and the origin and ρ_2 the distance between P and the point charge. The potential at P due to the point charge is [3]

$$\phi = \frac{1}{4\pi\epsilon} \frac{1}{\rho_2}. \quad (2.1)$$

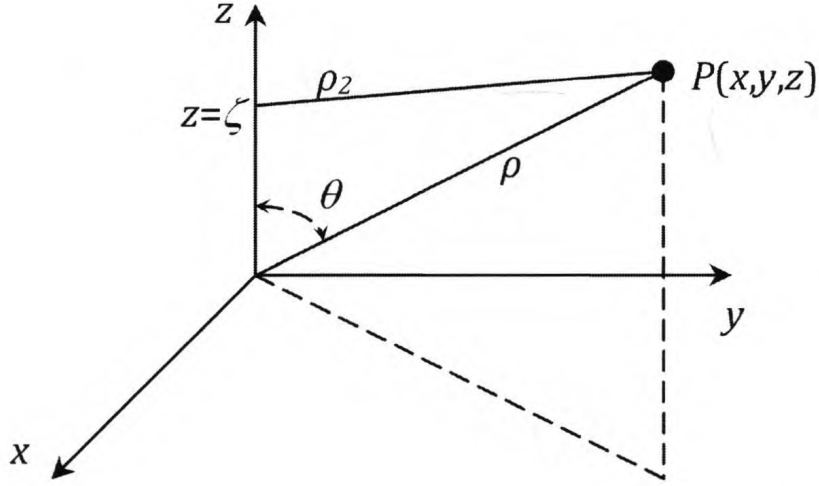


Figure 2.1: Graph showing the location of an arbitrary point P in relation to a point charge located on the z -axis at $z = \zeta$.

According to the Cosine Law,

$$\rho_2^2 = \rho^2 + \zeta^2 - 2\rho\zeta \cos \theta. \quad (2.2)$$

If we consider the inverse of the distance between the points $z = \zeta$ and P as a function of ζ ,

$$f(\zeta) = \frac{1}{\rho_2} = (\rho^2 + \zeta^2 - 2\rho\zeta \cos \theta)^{-\frac{1}{2}}. \quad (2.3)$$

Using a Taylor series at $\zeta = 0$, this function can be written as [4]

$$f(\zeta) = \sum_{n=0}^{\infty} \frac{\zeta^n}{n!} \left[\frac{\partial^n f(\zeta)}{\partial \zeta^n} \right]_{\zeta=0}.$$

From the geometry described in Figure 2.1, it is obvious that [5]

$$\frac{\partial}{\partial \zeta} \left(\frac{1}{\rho_2} \right) = -\frac{\partial}{\partial z} \left(\frac{1}{\rho_2} \right).$$

We make use of this equation because ρ is a function of z . Thus,

$$\left[\frac{\partial^n f(\zeta)}{\partial \zeta^n} \right]_{\zeta=0} = (-1)^n \left[\frac{\partial^n f(\zeta)}{\partial z^n} \right]_{\zeta=0}$$

and

$$f(\zeta) = \sum_{n=0}^{\infty} \frac{(-\zeta)^n}{n!} \left[\frac{\partial^n f(\zeta)}{\partial z^n} \right]_{\zeta=0}.$$

From (2.3),

$$f(0) = \frac{1}{\rho}.$$

Thus,

$$f(\zeta) = \sum_{n=0}^{\infty} \frac{(-\zeta)^n}{n!} \frac{\partial^n}{\partial z^n} \left(\frac{1}{\rho} \right).$$

Combining this result with (2.1),

$$\phi = \frac{q}{4\pi\epsilon} \sum_{n=0}^{\infty} \frac{(-\zeta)^n}{n!} \frac{\partial^n}{\partial z^n} \left(\frac{1}{\rho} \right). \quad (2.4)$$

Using different methodology, a different equation can be reached for the potential at P . From (2.2), it follows that

$$\rho_2^2 = \rho^2 \left[1 + \left(\frac{\zeta}{\rho} \right)^2 - 2 \frac{\zeta}{\rho} \cos \theta \right]$$

and

$$\frac{1}{\rho_2} = \frac{1}{\rho} \left[1 + \left(\frac{\zeta}{\rho} \right)^2 - 2 \frac{\zeta}{\rho} \cos \theta \right]^{-\frac{1}{2}}.$$

Using the identity [6]

$$(1 - 2xt + t^2)^{-\frac{1}{2}} = \sum_{n=0}^{\infty} P_n(x) t^n,$$

we can write the expansion of $\frac{1}{\rho_2}$ as

$$\frac{1}{\rho_2} = \frac{1}{\rho} \sum_{n=0}^{\infty} P_n(\cos \theta) \left(\frac{\zeta}{\rho} \right)^n. \quad (2.5)$$

This is an important equation.

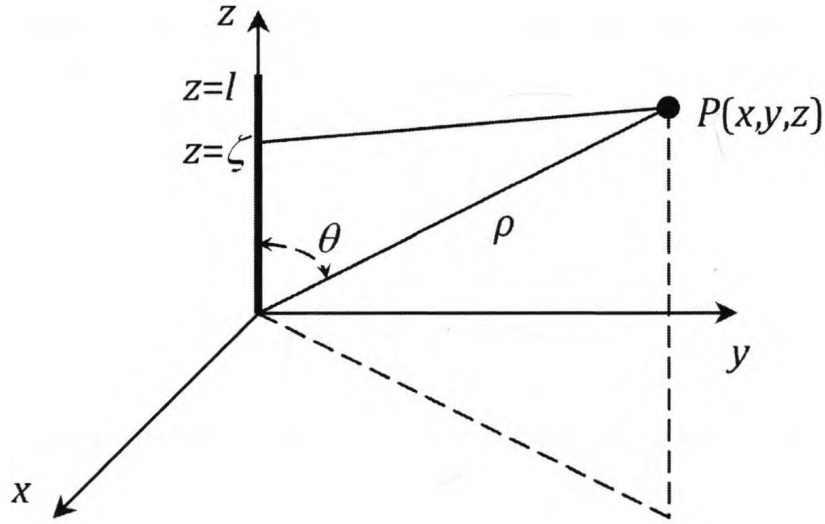


Figure 2.2: Graph showing the location of an arbitrary point P in relation to a line of charge that starts at the origin and ends at $z = l$.

Finally, we arrive at an alternative equation for the potential at P ,

$$\phi = \frac{1}{4\pi\epsilon} \frac{q}{\rho} \sum_{n=0}^{\infty} \frac{\zeta^n P_n(\cos \theta)}{\rho^n}. \quad (2.6)$$

All of these terms are equal to the corresponding terms in (2.4). Thus,

$$\frac{P_n(\cos \theta)}{\rho^{n+1}} = \frac{(-1)^n}{n!} \frac{\partial^n}{\partial z^n} \left(\frac{1}{\rho} \right). \quad (2.7)$$

2.1.2 Potential due to a Line of Charge

Figure 2.2 shows an arbitrary point P and a line of charge located on the z -axis from the origin to $z = l$. Let the charge density over this line be $\varrho(\zeta)$. Applying (2.6) to a very small element of the line of charge,

$$d\phi = \frac{\varrho(\zeta)}{4\pi\epsilon} \sum_{n=0}^{\infty} \frac{\zeta^n P_n(\cos \theta)}{\rho^{n+1}} d\zeta.$$

Thus, the potential at the arbitrary point due to the entire line of charge is [5]

$$\phi = \frac{1}{4\pi\epsilon} \sum_{n=0}^{\infty} \frac{P_n(\cos\theta)}{\rho^{n+1}} \int_0^l \varrho(\zeta) \zeta^n d\zeta. \quad (2.8)$$

The expression

$$p^{(n)} = \int_0^l \varrho(\zeta) \zeta^n d\zeta$$

is known as the axial multipole moment of n th order [5]. Thus, (2.8) can be written as

$$\phi = \frac{1}{4\pi\epsilon} \sum_{n=0}^{\infty} p^{(n)} \frac{P_n(\cos\theta)}{\rho^{n+1}}, \quad (2.9)$$

or using (2.7),

$$\phi = \frac{1}{4\pi\epsilon} \sum_{n=0}^{\infty} p^{(n)} \frac{(-1)^n}{n!} \frac{\partial^n}{\partial z^n} \left(\frac{1}{\rho} \right), \quad (2.10)$$

The leading term in this expansion is

$$\phi_0 = \frac{1}{4\pi\epsilon} p^{(0)} \frac{P_0(\cos\theta)}{\rho}. \quad (2.11)$$

Since [7]

$$P_0(\cos\theta) = 1,$$

this equation simplifies to

$$\phi_0 = \frac{1}{4\pi\epsilon} p^{(0)} \frac{1}{\rho}.$$

Let the total charge over this line of charge be q . Thus,

$$p^{(0)} = \int_0^l \varrho(\zeta) d\zeta = q$$

Finally, (2.11) simplifies to

$$\phi_0 = \frac{1}{4\pi\epsilon} \frac{q}{\rho}. \quad (2.12)$$

It is now apparent that the leading term of this expansion is equivalent to a point charge located at the origin with a charge of q . Assuming that this term is non-zero, this term is dominant for large ρ .

The second term in this expansion is

$$\phi_1 = \frac{1}{4\pi\epsilon} p^{(1)} \frac{P_1(\cos\theta)}{\rho^2}.$$

Since [7]

$$P_1(\cos\theta) = \cos\theta,$$

this equation simplifies to

$$\phi_1 = \frac{1}{4\pi\epsilon} p^{(1)} \frac{\cos\theta}{\rho^2}, \quad (2.13)$$

where

$$p^{(1)} = \int_0^l \varrho(\zeta) \zeta d\zeta$$

is known as the axial dipole moment. Generally, the first term in the expansion dominates for very large ρ . However, if there is no net charge, the first term will be zero and the second term will be dominant.

More generally, the first non-zero term in the expansion is dominant when $l \ll \rho$.

2.1.3 The Dipole Term

In the previous section, it was shown that the potential due to a line of charge can be approximated by the second term of the expansion ϕ_1 if the net charge over the line is zero and $l \ll \rho$. It was also shown that the first term in the expansion ϕ_0 is equivalent to a point charge located at the origin with a charge of q . In this section, we will find a configuration of point charges that is equivalent to the second term in the expansion ϕ_1 .

Let's consider the charge configuration shown in Figure 2.3. One point charge has

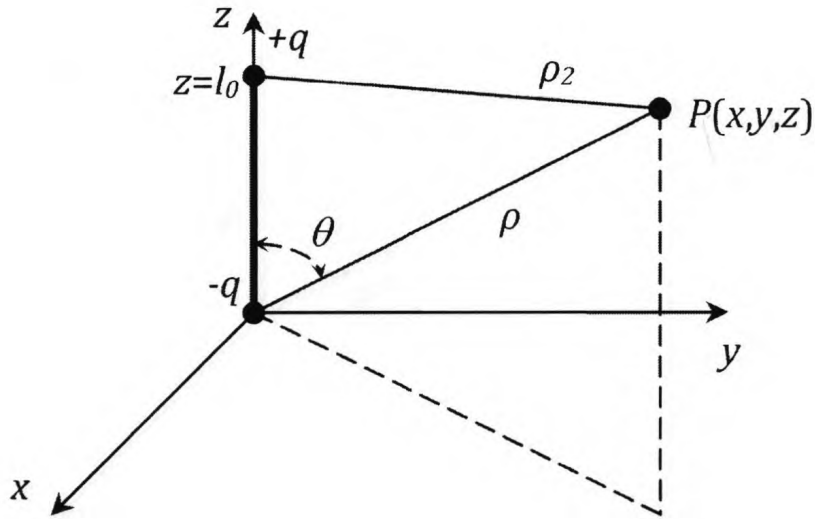


Figure 2.3: Graph showing the location of an arbitrary point P in relation to two point charges. One point charge has a charge of $-q$ and is located at the origin. The other point charge has a charge of $+q$ and is located on the z -axis at $z = l_0$.

a charge of $-q$ and is located at the origin. The other point charge has a charge of $+q$ and is located on the z -axis at $z = l_0$. The potential at an arbitrary point P due to these point charges is

$$\phi = \frac{1}{4\pi\epsilon} \frac{q}{\rho_2} - \frac{1}{4\pi\epsilon} \frac{q}{\rho} = \frac{q}{4\pi\epsilon} \left(\frac{1}{\rho_2} - \frac{1}{\rho} \right).$$

Assuming that $l_0 \ll \rho$, the second term of the multipole expansion will sufficiently approximate the potential at an arbitrary point because the total charge in the system is zero. Using (2.5) and ignoring all of the terms except the second term, the second term of the multipole expansion is

$$\phi_1 = \frac{q}{4\pi\epsilon} \left(\frac{1}{\rho} P_1(\cos\theta) \frac{l_0}{\rho} - \frac{1}{\rho} P_1(\cos\theta) \frac{0}{\rho} \right) = \frac{ql_0 \cos\theta}{4\pi\epsilon \rho^2}. \quad (2.14)$$

Referring to (2.13), it is evident that

$$ql_0 = p^{(1)}.$$

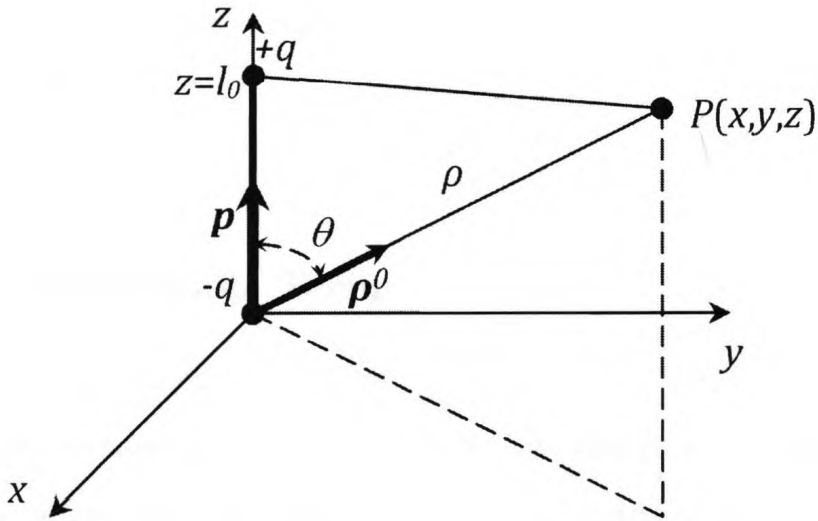


Figure 2.4: Graph showing the vectors that can be used to rewrite (2.14). \mathbf{p} is directed along the z -axis from the origin towards the positive point charge and has a magnitude of ql_0 . $\boldsymbol{\rho}^0$ is a unit vector directed from the origin towards the arbitrary point.

If q is allowed to approach infinity and l_0 is allowed to approach zero in such a manner that the product $p^{(1)}$ remains constant, (2.14) will apply everywhere except at the origin. Using (2.7), we can rewrite (2.14) as

$$\phi_1 = \frac{p^{(1)}}{4\pi\epsilon} \frac{\partial}{\partial z} \left(\frac{1}{\rho} \right).$$

We can also rewrite (2.14) using vectors. Let \mathbf{p} be a vector directed along the z -axis from the origin towards the positive point charge and let the magnitude of this vector be ql_0 . Let $\boldsymbol{\rho}^0$ be a unit vector directed from the origin towards the arbitrary point. These vectors are illustrated in Figure 2.4. The second term can be written as

$$\phi_1 = \frac{1}{4\pi\epsilon} \frac{\mathbf{p} \cdot \boldsymbol{\rho}^0}{\rho^2}.$$

Since

$$\nabla \left(\frac{1}{\rho} \right) = -\frac{1}{\rho^2} \boldsymbol{\rho}^0,$$

the second term can also be written as

$$\phi_1 = \frac{1}{4\pi\epsilon} \mathbf{p} \cdot \nabla \left(\frac{1}{\rho} \right).$$

2.1.4 The Quadrupole Term

In this section, we will describe a configuration of dipoles that is equivalent to the third term in the expansion ϕ_2 . Let's consider the charge configuration shown in Figure 2.5. One dipole has a moment of $-p^{(1)}$ and is located at the origin. The other dipole has a moment of $+p^{(1)}$ and is located at $z = l_1$. The potential at an arbitrary point P due to these dipoles is [5]

$$\phi_2 = \frac{1}{4\pi\epsilon} p^{(1)} l_1 \frac{\partial^2}{\partial z^2} \left(\frac{1}{\rho} \right) \quad (2.15)$$

Referring to (2.10), it is evident that

$$p^{(2)} = 2p^{(1)}l_1 = 2ql_0l_1$$

where l_0 is the distance between the two point charges within each dipole. Thus, (2.15) can be written as

$$\phi_2 = \frac{1}{4\pi\epsilon} \frac{p^{(2)}}{2!} \frac{\partial^2}{\partial z^2} \left(\frac{1}{\rho} \right) \quad (2.16)$$

If q is allowed to approach infinity and both l_0 and l_1 are allowed to approach zero in such a manner that the product $p^{(2)}$ remains constant, (2.16) will apply everywhere except at the origin.

2.1.5 Higher Order Terms

In this section, we will describe configurations of charges that are equivalent to higher order terms in the expansion ϕ_n . Let's consider the charge configuration shown in

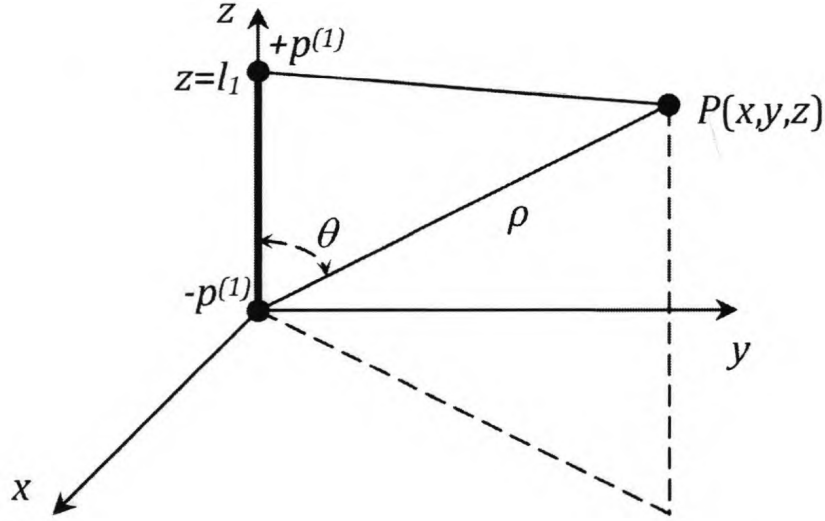


Figure 2.5: Graph showing the location of an arbitrary point P in relation to two dipoles. One dipole has a moment of $-p^{(1)}$ and is located at the origin. The other dipole has a moment of $+p^{(1)}$ and is located on the z -axis at $z = l_1$.

Figure 2.6. One multipole of order $n - 1$ has a moment of $-p^{(n-1)}$ and is located at the origin. The other multipole of order $n - 1$ has a moment of $+p^{(n-1)}$ and is located at $z = l_n$. The potential at an arbitrary point P due to these multipoles is [5]

$$\phi_n = \frac{(-1)^n p^{(n-1)} l_{n-1}}{4\pi\epsilon} \frac{\partial^n}{\partial z^n} \left(\frac{1}{\rho} \right) \quad (2.17)$$

Referring to (2.10), it is evident that

$$p^{(n)} = n p^{(n-1)} l_{n-1}$$

Thus, (2.17) can be written as

$$\phi_n = \frac{p^{(n)} (-1)^n}{4\pi\epsilon} \frac{\partial^n}{\partial z^n} \left(\frac{1}{\rho} \right), \quad n = 0, 1, \dots \quad (2.18)$$

If $p^{(n-1)}$ is allowed to approach infinity and l_{n-1} is allowed to approach zero in such a manner that the product $p^{(n)}$ remains constant, (2.18) will apply everywhere except at the origin.

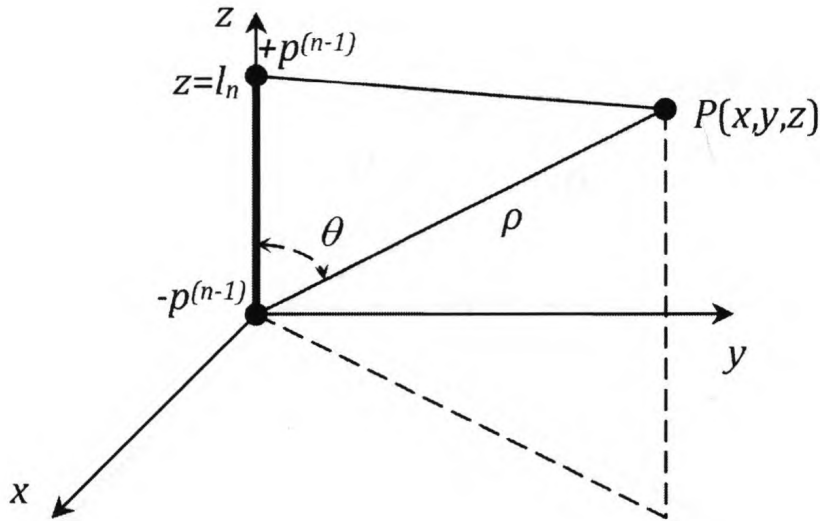


Figure 2.6: Graph showing the location of an arbitrary point P in relation to two multipoles of order $n - 1$. One multipole has a moment of $-p^{(n-1)}$ and is located at the origin. The other multipole has a moment of $+p^{(n-1)}$ and is located on the z -axis at $z = l_n$.

2.2 General Multipoles

Section 2.1 on axial multipoles considered charge distributions located on the z -axis only. This section on general multipoles considers more general charge distributions, for which, vector notation is needed.

We will consider the potential due to an arbitrary charge distribution. This charge distribution is located inside a sphere with a radius of R that is centered at the origin. We consider the potential at a point P that is arbitrarily located outside of the sphere. Figure 2.7 shows the arbitrary point P and a differential element of charge dq located arbitrarily within the sphere. Let $\boldsymbol{\rho}$ be the vector from the origin to P . Let $\boldsymbol{\rho}_1 = \xi\mathbf{i} + \eta\mathbf{j} + \zeta\mathbf{k}$ be the vector from the origin to dq . Let $\boldsymbol{\rho}_2$ be the vector from dq to P . The potential at P due to the differential element of charge is

$$d\phi = \frac{1}{4\pi\epsilon} \frac{dq}{|\boldsymbol{\rho}_2|}.$$

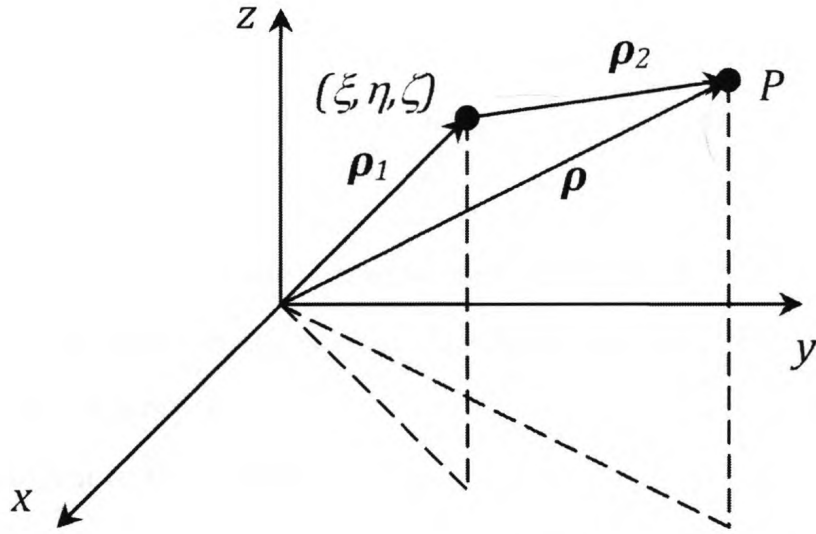


Figure 2.7: Graph showing the location of a point P that is arbitrarily located outside of the sphere. A differential element of charge dq is located arbitrarily inside the sphere. $\boldsymbol{\rho}$ is the vector from the origin to P . $\boldsymbol{\rho}_1 = \xi\mathbf{i} + \eta\mathbf{j} + \zeta\mathbf{k}$ is the vector from the origin to dq . $\boldsymbol{\rho}_2$ is the vector from dq to P .

Based on the assumption that $|\boldsymbol{\rho}_1| \ll |\boldsymbol{\rho}|$,

$$\boldsymbol{\rho}_2 \approx \boldsymbol{\rho}_1 + \boldsymbol{\rho}.$$

Therefore,

$$d\phi = \frac{1}{4\pi\epsilon} \frac{dq}{|\boldsymbol{\rho}_1 + \boldsymbol{\rho}|} = \frac{1}{4\pi\epsilon} \frac{\rho dv}{|\boldsymbol{\rho}_1 + \boldsymbol{\rho}|}.$$

Using a Taylor Series with $f(\mathbf{z}) = \frac{1}{|\mathbf{z}|}$ [8],

$$d\phi = \frac{1}{4\pi\epsilon} \rho dv \left[\frac{1}{|\boldsymbol{\rho}|} - \boldsymbol{\rho}_1 \cdot \nabla \left(\frac{1}{|\boldsymbol{\rho}|} \right) + \frac{1}{2} \boldsymbol{\rho}_1 \cdot \left(\boldsymbol{\rho}_1 \cdot \nabla \nabla \left(\frac{1}{|\boldsymbol{\rho}|} \right) \right) + \dots \right].$$

Integrating over the entire sphere,

$$\phi = \sum_{n=0}^{\infty} \phi_n = \frac{1}{4\pi\epsilon} \int \rho \left[\frac{1}{|\boldsymbol{\rho}|} - \boldsymbol{\rho}_1 \cdot \nabla \left(\frac{1}{|\boldsymbol{\rho}|} \right) + \frac{1}{2} \boldsymbol{\rho}_1 \cdot \left(\boldsymbol{\rho}_1 \cdot \nabla \nabla \left(\frac{1}{|\boldsymbol{\rho}|} \right) \right) + \dots \right] dv.$$

The leading term in the expansion is

$$\phi_0 = \frac{1}{4\pi\epsilon} \frac{1}{|\boldsymbol{\rho}|} \int \varrho dv.$$

This term is equivalent to a point charge located at the origin with a charge equal to the total charge contained in the sphere. Assuming that this term is non-zero, this term is dominant for large $|\boldsymbol{\rho}|$.

The second term in the expansion is

$$\phi_1 = -\frac{1}{4\pi\epsilon} \int \varrho \boldsymbol{\rho}_1 \cdot \nabla \left(\frac{1}{|\boldsymbol{\rho}|} \right) dv. = -\frac{1}{4\pi\epsilon} \int \varrho \begin{bmatrix} \xi \\ \eta \\ \zeta \end{bmatrix} \cdot \begin{bmatrix} \frac{\partial}{\partial x} \left(\frac{1}{|\boldsymbol{\rho}|} \right) \\ \frac{\partial}{\partial y} \left(\frac{1}{|\boldsymbol{\rho}|} \right) \\ \frac{\partial}{\partial z} \left(\frac{1}{|\boldsymbol{\rho}|} \right) \end{bmatrix} dv.$$

This term is equivalent to the potential generated by a dipole located at the origin. The dipole term sufficiently approximates the potential for large $|\boldsymbol{\rho}|$ if it is non-zero and there is no net charge in the sphere.

The third term in the expansion is

$$\begin{aligned} \phi_2 &= \frac{1}{4\pi\epsilon} \frac{1}{2} \int \varrho \boldsymbol{\rho}_1 \cdot \left(\boldsymbol{\rho}_1 \cdot \nabla \nabla \left(\frac{1}{|\boldsymbol{\rho}|} \right) \right) dv \\ &= \frac{1}{4\pi\epsilon} \frac{1}{2} \int \varrho \begin{bmatrix} \xi \\ \eta \\ \zeta \end{bmatrix} \cdot \left(\begin{bmatrix} \xi \\ \eta \\ \zeta \end{bmatrix} \cdot \begin{bmatrix} \frac{\partial^2}{\partial x^2} \left(\frac{1}{|\boldsymbol{\rho}|} \right) & \frac{\partial^2}{\partial x \partial y} \left(\frac{1}{|\boldsymbol{\rho}|} \right) & \frac{\partial^2}{\partial x \partial z} \left(\frac{1}{|\boldsymbol{\rho}|} \right) \\ \frac{\partial^2}{\partial y \partial x} \left(\frac{1}{|\boldsymbol{\rho}|} \right) & \frac{\partial^2}{\partial y^2} \left(\frac{1}{|\boldsymbol{\rho}|} \right) & \frac{\partial^2}{\partial y \partial z} \left(\frac{1}{|\boldsymbol{\rho}|} \right) \\ \frac{\partial^2}{\partial z \partial x} \left(\frac{1}{|\boldsymbol{\rho}|} \right) & \frac{\partial^2}{\partial z \partial y} \left(\frac{1}{|\boldsymbol{\rho}|} \right) & \frac{\partial^2}{\partial z^2} \left(\frac{1}{|\boldsymbol{\rho}|} \right) \end{bmatrix} \right) dv. \end{aligned}$$

This term is equivalent to the potential generated by a quadrupole located at the origin. The quadrupole term sufficiently approximates the potential for large $|\boldsymbol{\rho}|$ if it is non-zero and the first two terms in the expansion are zero.

The dipole term included the expression $\nabla \left(\frac{1}{|\boldsymbol{\rho}|} \right)$ which is a tensor of first rank. Likewise, the quadrupole term included the expression $\nabla \nabla \left(\frac{1}{|\boldsymbol{\rho}|} \right)$ which is a tensor of second rank. In general, higher order terms ϕ_n will include tensors of rank n .

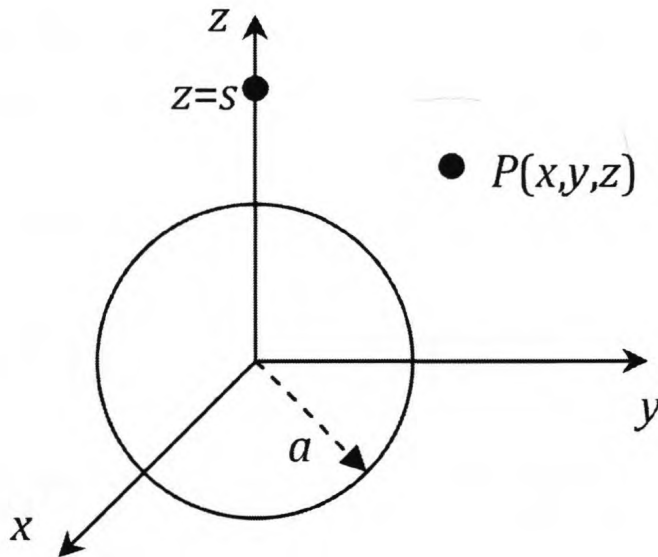


Figure 2.8: Graph showing a grounded sphere with a radius of a that is centered at the origin, a point charge with a magnitude of q that is located on the z -axis at $z = s$ where $a < s$, and a point P that is arbitrarily located outside of the sphere.

Similarly to the dipole and quadrupole terms, these higher order terms will include the necessary number of dot product operations to ultimately reduce the tensor to a scalar.

The first non-zero term in the expansion is dominant when $R \ll |\rho|$.

2.3 Solving Electrostatic Problems with Multipoles

2.3.1 Method of Images for a Grounded Sphere

Figure 2.8 shows a grounded sphere with a radius of a that is centered at the origin, a point charge with a magnitude of q that is located on the z -axis at $z = s$ where $a < s$, and a point P that is arbitrarily located outside of the sphere. In this section, we will find the potential at P due to the grounded sphere and the point charge.

This can be easily accomplished using the Method of Images [9]. Suppose a point charge is placed on the z -axis at $z = b = \frac{a^2}{s}$. This charge is referred to as the image

charge. Let the magnitude of the image charge be $-q\frac{b}{a}$. This configuration is shown in Figure 2.9. The potential at P due to both charges is [3]

$$\begin{aligned}\phi &= \frac{1}{4\pi\epsilon} \frac{q}{\sqrt{x^2 + y^2 + (z-s)^2}} + \frac{1}{4\pi\epsilon} \frac{-q\frac{b}{a}}{\sqrt{x^2 + y^2 + (z-b)^2}} \\ &= \frac{1}{4\pi\epsilon} q \left[\frac{1}{\sqrt{x^2 + y^2 + (z-s)^2}} - \frac{a}{s\sqrt{x^2 + y^2 + (z-\frac{a^2}{s})^2}} \right] \\ &= \frac{1}{4\pi\epsilon} q \left[\frac{1}{\sqrt{x^2 + y^2 + z^2 - 2zs + s^2}} - \frac{a}{s\sqrt{x^2 + y^2 + z^2 - 2z\frac{a^2}{s} + \frac{a^4}{s^2}}} \right].\end{aligned}$$

On the surface of the grounded sphere,

$$x^2 + y^2 + z^2 = a^2$$

and

$$\begin{aligned}\phi &= \frac{1}{4\pi\epsilon} q \left[\frac{1}{\sqrt{a^2 - 2zs + s^2}} - \frac{a}{s\sqrt{a^2 - 2z\frac{a^2}{s} + \frac{a^4}{s^2}}} \right] \\ &= \frac{1}{4\pi\epsilon} q \left[\frac{1}{\sqrt{a^2 - 2zs + s^2}} - \frac{1}{\sqrt{s^2 - 2zs + a^2}} \right] \\ &= 0.\end{aligned}$$

Thus, the potential on the surface of the sphere due to the actual charge and the image charge is zero. In a sense, the presence of the image charge mimics the presence of the grounded sphere for this configuration. Using the uniqueness theorem, one can prove that the potential at any point outside of the sphere is equal in both the configuration shown in Figure 2.8 and the configuration shown in Figure 2.9 [10].

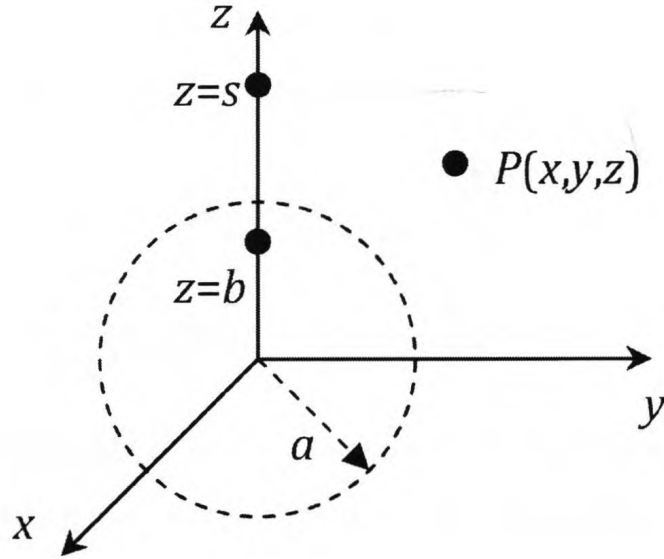


Figure 2.9: Graph showing a point charge with a magnitude of q that is located on the z -axis at $z = s$ where $a < s$, an image charge with a magnitude of $-q\frac{b}{a}$ that is located on the z -axis at $z = b = \frac{a^2}{s}$, and a point P that is arbitrarily located outside of the sphere.

2.3.2 Replacing an Image Charge with a Multipole

The image charge in Figure 2.9 can be replaced by a multipole located at the origin. This methodology was described in Section 2.1.1. In this case, the distance between the image charge and the arbitrary point is

$$\rho_2 = \sqrt{x^2 + y^2 + (z - b)^2}.$$

The potential at P due to the image charge is

$$\phi = -\frac{1}{4\pi\epsilon} q \frac{b}{a} \frac{1}{\rho_2}.$$

Using (2.5),

$$\phi = -\frac{1}{4\pi\epsilon} q \frac{b}{a} \frac{1}{\rho} \sum_{n=0}^{\infty} P_n(\cos\theta) \left(\frac{b}{\rho}\right)^n = -\frac{1}{4\pi\epsilon} q \frac{1}{a} \sum_{n=0}^{\infty} P_n(\cos\theta) \left(\frac{b}{\rho}\right)^{n+1}$$

where the variables θ and ρ are defined in Figure 2.1. Thus, the potential at P due to both the actual point charge and the multipole is

$$\begin{aligned}\phi &= \frac{1}{4\pi\epsilon} \frac{q}{\sqrt{x^2 + y^2 + (z-s)^2}} - \frac{1}{4\pi\epsilon} \frac{q}{a} \sum_{n=0}^{\infty} P_n(\cos\theta) \left(\frac{b}{\rho}\right)^{n+1} \\ &= \frac{1}{4\pi\epsilon} q \left[\frac{1}{\sqrt{x^2 + y^2 + (z-s)^2}} - \frac{1}{a} \sum_{n=0}^{\infty} P_n(\cos\theta) \left(\frac{b}{\rho}\right)^{n+1} \right].\end{aligned}$$

It may seem undesirable to replace a simple entity such as a point charge with a more complex entity such as a multipole. However, this methodology can be advantageous because the multipole is located at the origin, as opposed to the point charge which is located elsewhere.

2.4 Solution of the Laplace Equation in Spherical Coordinates

An alternative method for finding the potential due to an arbitrary charge distribution is to find the solution of the Laplace equation with the appropriate boundary conditions. In this section, we will accomplish this using separation of variables. Figure 2.10 illustrates the relationship between spherical coordinates and rectangular coordinates. In spherical coordinates, the Laplace equation is [7]

$$\nabla^2\phi = \frac{1}{\rho^2} \left[\frac{\partial}{\partial\rho} \left(\rho^2 \frac{\partial\phi}{\partial\rho} \right) + \frac{1}{\sin\theta} \frac{\partial}{\partial\theta} \left(\frac{\partial\phi}{\partial\theta} \sin\theta \right) + \frac{1}{\sin^2\theta} \frac{\partial^2\phi}{\partial\alpha^2} \right] = 0.$$

We will assume that the solution is axisymmetric, and therefore, independent of α . Thus, the solution can be represented by $\phi(\rho, \theta)$ and

$$\frac{\partial^2\phi}{\partial\alpha^2} = 0.$$

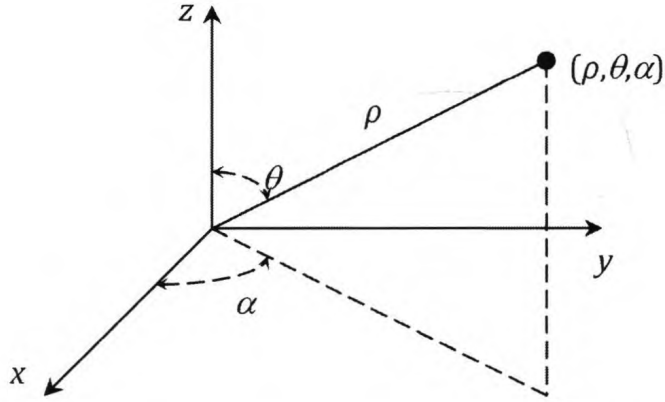


Figure 2.10: Graph showing the relationship between spherical coordinates and rectangular coordinates.

Therefore, the Laplace equation simplifies to

$$\frac{\partial}{\partial \rho} \left(\rho^2 \frac{\partial \phi}{\partial \rho} \right) + \frac{1}{\sin \theta} \frac{\partial}{\partial \theta} \left(\frac{\partial \phi}{\partial \theta} \sin \theta \right) = 0.$$

Substituting $\phi(\rho, \theta) = R(\rho)\Theta(\theta)$,

$$\frac{\partial}{\partial \rho} [\rho^2 R'(\rho)\Theta(\theta)] + \frac{1}{\sin \theta} \frac{\partial}{\partial \theta} [R(\rho)\Theta'(\theta) \sin \theta] = 0.$$

Expanding the first term and dividing the equation by $R(\rho)\Theta(\theta)$ yields

$$\frac{2\rho R'(\rho) + \rho^2 R''(\rho)}{R(\rho)} + \frac{1}{\Theta(\theta) \sin \theta} \frac{\partial}{\partial \theta} [\Theta'(\theta) \sin \theta] = 0.$$

Thus,

$$\frac{2\rho R'(\rho) + \rho^2 R''(\rho)}{R(\rho)} = -\frac{1}{\Theta(\theta) \sin \theta} \frac{\partial}{\partial \theta} [\Theta'(\theta) \sin \theta] = \lambda$$

where λ is known as the separation constant. Therefore,

$$\rho^2 R''(\rho) + 2\rho R'(\rho) - \lambda R(\rho) = 0 \tag{2.19}$$

and

$$\frac{\partial}{\partial \theta} [\Theta'(\theta) \sin \theta] + \lambda \Theta(\theta) \sin \theta = 0. \quad (2.20)$$

Substituting $x = \cos \theta$ and $y(x) = \Theta(\arccos x) = \Theta(\theta)$ for $-1 \leq x \leq 1$ in (2.20) yields the Legendre equation [7]

$$(1 - x^2)y'' - 2xy' + \lambda y = 0$$

This equation has a valid solution only if [7]

$$\lambda = n(n + 1) \text{ for } n = 0, 1, 2, \dots$$

and this solution is a constant multiple of the Legendre polynomial [7]

$$\Theta_n(\theta) = P_n(x) = P_n(\cos \theta).$$

Since the valid separation constants are now known, (2.19) can now be written as

$$\rho^2 R''(\rho) + 2\rho R'(\rho) - n(n + 1)R(\rho) = 0$$

Substituting the trial solution

$$R(\rho) = \rho^k$$

yields

$$k^2 + k - n(n + 1) = 0.$$

The solution is

$$k = -n - 1, n.$$

Therefore, the general solution for $R(\rho)$ is

$$R(\rho) = A\rho^n + \frac{B}{\rho^{n+1}}$$

If the given problem requires continuity at $\rho = 0$, then $B = 0$. If the given problem requires the solution to be bounded as ρ approaches infinity, then $A = 0$. If the given problem imposes neither of these conditions, then both of these terms must be retained. The formal series solution is

$$\phi(\rho, \theta) = \sum_{n=0}^{\infty} P_n(\cos \theta) \left(A_n \rho^n + \frac{B_n}{\rho^{n+1}} \right).$$

This solution is remarkably similar to the multipole expansion for the potential due to a line of charge given in (2.9). In fact, if

$$A_n = 0 \quad \text{and} \quad B_n = \frac{1}{4\pi\epsilon} p^{(n)},$$

then this result becomes identical to (2.9). Note that, in this case, $A_n = 0$ because the solution must be bounded as $\rho \rightarrow \infty$. Solving the Laplace equation in spherical coordinates and finding the coefficients A_n and B_n for a given set of boundary conditions is equivalent to finding the multipole moments for a given charge distribution.

2.5 Solution of the Laplace Equation in Cylindrical Coordinates

In this section, we will use separation of variables to find the solution of the Laplace equation in cylindrical coordinates. Figure 2.11 illustrates the relationship between cylindrical coordinates and rectangular coordinates. In cylindrical coordinates, the

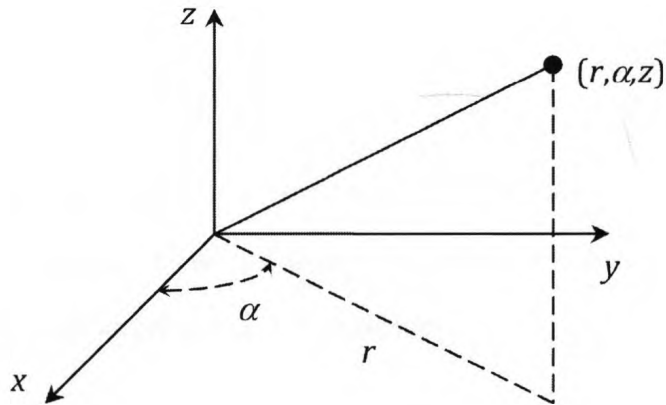


Figure 2.11: Graph showing the relationship between cylindrical coordinates and rectangular coordinates.

Laplace equation is [7]

$$\nabla^2 \phi = \frac{\partial^2 \phi}{\partial r^2} + \frac{1}{r} \frac{\partial \phi}{\partial r} + \frac{1}{r^2} \frac{\partial^2 \phi}{\partial \alpha^2} + \frac{\partial^2 \phi}{\partial z^2} = 0. \quad (2.21)$$

We will assume that the solution is axisymmetric, and therefore, independent of α . Thus, the solution can be represented by $\phi(r, z)$ and

$$\frac{\partial^2 \phi}{\partial \alpha^2} = 0.$$

Therefore, the Laplace equation simplifies to

$$\frac{\partial^2 \phi}{\partial r^2} + \frac{1}{r} \frac{\partial \phi}{\partial r} + \frac{\partial^2 \phi}{\partial z^2} = 0.$$

Substituting $\phi(r, z) = R(r)Z(z)$,

$$R''(r)Z(z) + \frac{1}{r}R'(r)Z(z) + R(r)Z''(z) = 0.$$

Dividing the equation by $R(r)Z(z)$ yields

$$\frac{R''(r) + \frac{1}{r}R'(r)}{R(r)} + \frac{Z''(z)}{Z(z)} = 0.$$

Thus,

$$\frac{R''(r) + \frac{1}{r}R'(r)}{R(r)} = -\frac{Z''(z)}{Z(z)} = \lambda.$$

where λ is known as the separation constant. In this case, $(-\lambda)$ can optionally be used in place of λ . Using $(-\lambda)$ would lead to a differently expressed solution that is equally valid. We will proceed using λ . Therefore,

$$R''(r) + \frac{1}{r}R'(r) - \lambda R(r) = 0 \quad (2.22)$$

and

$$Z''(z) + \lambda Z(z) = 0. \quad (2.23)$$

(2.22) is the modified Bessel equation of order 0. Its solution is

$$R(r) = QI_0(\lambda r) + BK_0(\lambda r).$$

The solution of (2.23) is

$$Z(z) = C \sin(\lambda z) + D \cos(\lambda z).$$

Therefore,

$$\phi(r, z) = \int_0^\infty [Q(t)I_0(tr) + B(t)K_0(tr)][C(t) \sin(tz) + D(t) \cos(tz)] dt.$$

To use this solution to solve a boundary value problem, one would rely on the boundary conditions to find the arbitrary functions $Q(t)$, $B(t)$, $C(t)$, and $D(t)$.

If

$$B(t)D(t) = \frac{q}{2\pi^2\epsilon} \quad \text{and} \quad C(t) = Q(t) = 0,$$

then

$$\phi(r, z) = \int_0^\infty \frac{q}{2\pi^2\epsilon} K_0(rt) \cos(zt) dt.$$

Using the identity [11]

$$\int_0^\infty K_0(rt) \cos(zt) dt = \frac{\pi}{2\sqrt{z^2 + r^2}},$$

we can write

$$\phi(r, z) = \frac{q}{2\pi^2\epsilon} \frac{\pi}{2\sqrt{z^2 + r^2}} = \frac{1}{4\pi\epsilon} \frac{q}{\rho}.$$

This is identical to the potential due to a point charge located at the origin (2.12), or in other words, the first term in the multipole expansion of a given charge distribution.

If

$$C(t) = -\frac{2t}{\pi}, \quad Q(t) = \frac{K_1(t)}{I_1(t)}, \quad B(t) = 1, \quad \text{and} \quad D(t) = 0,$$

then

$$\phi(r, z) = \int_0^\infty -\frac{2t}{\pi} \left[\frac{K_1(t)}{I_1(t)} I_0(tr) + K_0(tr) \right] \sin(tz) dt$$

This is equivalent to the potential of a unit dipole [12] and corresponds with the second term in the multipole expansion of a given charge distribution.

Like in the case of spherical coordinates, solving the Laplace equation in cylindrical coordinates and finding the arbitrary functions $Q(t)$, $B(t)$, $C(t)$, and $D(t)$ for a given set of boundary conditions is equivalent to finding the multipole moments for a given charge distribution.

Chapter 3

The Potential around a Sphere inside a Cylinder

We have discussed how, in the context of electromagnetics, an arbitrary charge distribution can be replaced with a multipole expansion where the multipole expansion consists of a collection of point charges. Similarly, multipole expansions can be utilized in fluid mechanics. However, in the context of fluid mechanics, a multipole expansion consists of a collection of fluid sources and fluid sinks.

The solution presented in this chapter is partly based on the method of Linton [2], which in turn was based on earlier work [13, 14, 15, 16]. The asymptotic analysis was guided by a roughly similar calculation [17]. The difficulty with this geometry arises from the fact that there is no orthogonal system in which both spherical and cylindrical coordinates fit, so the usual method of separation of variables cannot be applied.

Linton [2] uses the method of multipoles to derive a general solution. This consists of constructing a set of functions that satisfy the governing (Laplace) equation and all the boundary conditions except the one on the sphere and representing the solution as a superposition of them. The condition on the sphere leads to an infinite set of

linear equations in the coefficients of the solution. A similar approach is given by Smythe [16], who studies the vector potential for the problem, instead of the scalar potential, but he also obtains an infinite system of equations. The first new feature of this thesis is the replacing of Smythe's numerical solution of the system of equations with a more symbolic one. Our method expresses the unknown coefficients as series expansions in the ratio sphere radius to cylinder radius. While the numerical approach of Smythe must be repeated for each ratio, our symbolic solution is valid for all ratios.

The symbolic solution also allows an analysis of the singular behaviour when the sphere is almost the same diameter as the cylinder. In this case, we first obtain an asymptotic solution by matching approximations in the gap between sphere and cylinder with the field outside the gap. Because both solutions (the multipole one and the asymptotic one) are expressed symbolically, they can be matched and hence verified and used to improve convergence.

The first coefficient of the multipole representation has an important practical interest, being connected with the increase in the resistance of the cylinder for the electrical problem, or the effective increase of the tube length in the fluid problem, due to the insertion of the sphere. Our results agree well with the results computed by Smythe for different ratios.

3.1 Solution of Sphere Problem

We consider the potential around a sphere of radius a situated on the axis of a circular tube of radius d . We use a cylindrical coordinate system (r, z, α) and a spherical coordinate system (ρ, θ, α) , both of which have their origins at the centre of the sphere and are scaled so that the boundary of the cylinder corresponds to $r = 1$. The spherical boundary is then given by $\rho = \lambda$ where λ is the ratio of the sphere radius to the cylinder radius. Note that this instance of λ has no connection with

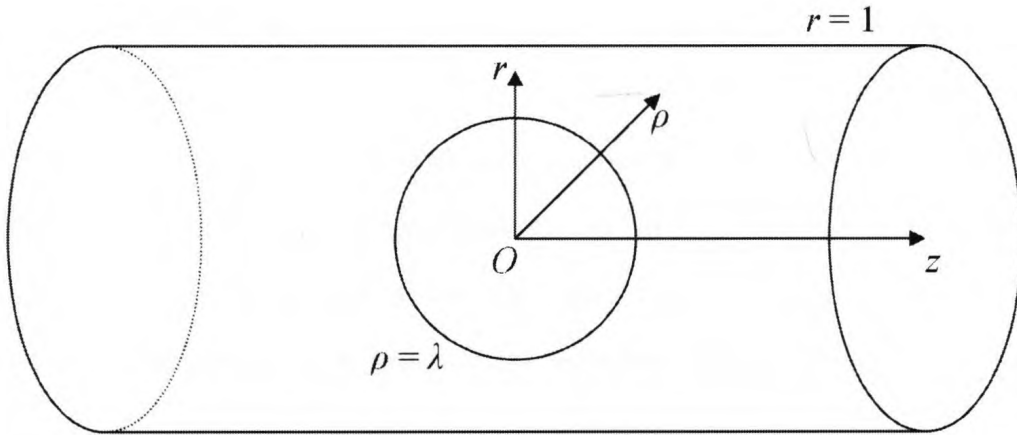


Figure 3.1: The coordinate systems for the sphere inside the cylinder.

the instances of λ in the previous chapter. The axial symmetry is used to suppress reference to the azimuthal angle α . This coordinate system is illustrated in Figure 3.1. The two systems of coordinates are connected by the relations

$$\begin{aligned} z &= \rho \cos \theta, \\ r &= \rho \sin \theta. \end{aligned}$$

Far from the sphere, the potential tends to Vz , which can be interpreted as a uniform applied field, whether a velocity field or electric field. We introduce the velocity potential in the form $Vz + \phi$. The disturbance potential ϕ must satisfy the Laplace equation in cylindrical coordinates

$$\frac{1}{r} \frac{\partial}{\partial r} \left(r \frac{\partial \phi}{\partial r} \right) + \frac{\partial^2 \phi}{\partial z^2} = 0$$

together with the boundary conditions

$$\frac{\partial \phi}{\partial r} = 0 \quad \text{on} \quad r = 1, \tag{3.1}$$

$$\frac{\partial \phi}{\partial \rho} = -V \cos \theta \quad \text{on} \quad \rho = \lambda, \tag{3.2}$$

$$\frac{\partial \phi}{\partial z} \rightarrow 0 \quad \text{as} \quad |z| \rightarrow \infty. \tag{3.3}$$

The latter equation applies both when $z \rightarrow -\infty$ and when $z \rightarrow +\infty$. Therefore, $\phi \rightarrow \eta_1$ as $z \rightarrow -\infty$ and $\phi \rightarrow \eta$ as $z \rightarrow +\infty$ where η_1 and η are unknown constants. Since there is no net charge in the cylinder, according to Gauss' Law, there must be no net flux at the boundaries of the cylinder. According to (3.1), there is no flux at $r = 1$. Therefore, the total flux across the top of the cylinder must be equal to the negative total flux across the bottom of the cylinder. Therefore, $\eta = -\eta_1$ and

$$\phi \rightarrow \eta \operatorname{sgn}(z) \quad \text{as} \quad |z| \rightarrow \infty. \quad (3.4)$$

where η depends on λ and is, in general, non-zero.

To solve the problem above we use dual expansions. First, we express the solution in cylindrical coordinates as a linear combination of functions satisfying the equation and all the boundary conditions but the one on the sphere. Then, we transform the solution in spherical coordinates and apply the condition on the sphere (see [2]).

In Section 2.5, we used separation of variables to solve the Laplace equation in cylindrical coordinates and we found that

$$\phi(r, z) = R(r)Z(z)$$

where

$$R(r) = Q(t)I_0(tr) + B(t)K_0(tr)$$

and

$$Z(z) = C(t) \sin(tz) + D(t) \cos(tz).$$

We start by applying the boundary condition (3.1).

$$R'(r) = -Q(t)tI_1(tr) + B(t)tK_1(tr).$$

Applying the boundary condition at $r = 1$,

$$R'(1) = -Q(t)tI_1(t) + B(t)tK_1(t) = 0.$$

Therefore,

$$Q(t) = B(t) \frac{K_1(t)}{I_1(t)}$$

and

$$R(r) = B(t) \left[\frac{K_1(t)}{I_1(t)} I_0(tr) + K_0(tr) \right].$$

The potential function is antisymmetric in Z . Therefore, $Z(z)$ must be an odd function, $D = 0$, and

$$Z(z) = C(t) \sin(tz).$$

Therefore,

$$\phi(r, z) = \int_0^\infty H(t) \left[\frac{K_1(t)}{I_1(t)} I_0(tr) + K_0(tr) \right] \sin(tz) dt \quad (3.5)$$

where H is a newly defined arbitrary function.

From Section 2.4, the solution of the Laplace equation in spherical coordinates is

$$\phi(\rho, \theta) = \sum_{n=0}^{\infty} P_n(\cos \theta) \left(L_n \rho^n + \frac{M_n}{\rho^{n+1}} \right).$$

where L_n and M_n are the arbitrary constants.

Since $z = \rho \cos(\theta)$, $\phi(-z) = -\phi(z)$. Since the problem is symmetric in z ,

$$-z = \rho \cos(\pi - \theta) = -\rho \cos(\theta)$$

and

$$P_{2n}(\cos \theta) \left(L_{2n} \rho^{2n} + \frac{M_{2n}}{\rho^{2n+1}} \right) = P_{2n}(-\cos \theta) \left(L_{2n} \rho^{2n} + \frac{M_{2n}}{\rho^{2n+1}} \right)$$

which is true only if L_{2n} and M_{2n} is zero. Thus we have eliminated half of the terms

and

$$\phi(\rho, \theta) = \sum_{n=1}^{\infty} P_{2n-1}(\cos \theta) \left(L_{2n-1} \rho^{2n-1} + \frac{M_{2n-1}}{\rho^{2n}} \right). \quad (3.6)$$

Using the identity [18]

$$\frac{P_{2n-1}(\cos \theta)}{\rho^{2n}} = \frac{2(-1)^{n+1}}{\pi(2n-1)!} \int_0^{\infty} t^{2n-1} K_0(tr) \sin(tz) dt,$$

we can write

$$\sum_{n=1}^{\infty} P_{2n-1}(\cos \theta) \frac{M_{2n-1}}{\rho^{2n}} = \sum_{n=1}^{\infty} M_{2n-1} \frac{2(-1)^{n+1}}{\pi(2n-1)!} \int_0^{\infty} t^{2n-1} K_0(tr) \sin(tz) dt.$$

It can be proven that the order of summation and integration may be swapped in this case. Thus,

$$\sum_{n=1}^{\infty} P_{2n-1}(\cos \theta) \frac{M_{2n-1}}{\rho^{2n}} = \int_0^{\infty} \sum_{n=1}^{\infty} M_{2n-1} \frac{2(-1)^{n+1}}{\pi(2n-1)!} t^{2n-1} K_0(tr) \sin(tz) dt.$$

By combining this equation with (3.5), it is clear that

$$H(t) = \sum_{n=1}^{\infty} M_{2n-1} \frac{2(-1)^{n+1}}{\pi(2n-1)!} t^{2n-1}$$

and

$$\phi(r, z) = \int_0^{\infty} \sum_{n=1}^{\infty} M_{2n-1} \frac{2(-1)^{n+1}}{\pi(2n-1)!} t^{2n-1} \left[\frac{K_1(t)}{I_1(t)} I_0(tr) + K_0(tr) \right] \sin(tz) dt.$$

Reversing the order of summation and integration again,

$$\phi(r, z) = \sum_{n=1}^{\infty} M_{2n-1} \int_0^{\infty} \frac{2(-1)^{n+1}}{\pi(2n-1)!} t^{2n-1} \left[\frac{K_1(t)}{I_1(t)} I_0(tr) + K_0(tr) \right] \sin(tz) dt. \quad (3.7)$$

Using the identity [18]

$$I_0(tr) \sin(tz) = \sum_{m=1}^{\infty} \frac{(-1)^{m+1}}{(2m-1)!} (t\rho)^{2m-1} P_{2m-1}(\cos \theta),$$

$$\begin{aligned} \phi(r, z) = & \sum_{n=1}^{\infty} M_{2n-1} \int_0^{\infty} \frac{2(-1)^{n+1}}{\pi(2n-1)!} t^{2n-1} \\ & \left[\frac{K_1(t)}{I_1(t)} \sum_{m=1}^{\infty} \frac{(-1)^{m+1}}{(2m-1)!} (t\rho)^{2m-1} P_{2m-1}(\cos \theta) + K_0(tr) \sin(tz) \right] dt. \end{aligned}$$

Now, (3.6) can be written as

$$\begin{aligned} \phi(\rho, \theta) = & \sum_{n=1}^{\infty} M_{2n-1} \frac{P_{2n-1}(\cos \theta)}{\rho^{2n}} \\ & + \sum_{n=1}^{\infty} \sum_{m=1}^{\infty} M_{2n-1} \frac{2(-1)^{n+1}}{\pi(2n-1)!} \frac{(-1)^{m+1}}{(2m-1)!} \rho^{2m-1} P_{2m-1}(\cos \theta) \int_0^{\infty} t^{2n-1} \frac{K_1(t)}{I_1(t)} t^{2m-1} dt. \end{aligned}$$

Next, we find the partial derivative

$$\begin{aligned} \frac{\partial}{\partial \rho} \phi(\rho, \theta) = & \sum_{n=1}^{\infty} M_{2n-1} \frac{-2nP_{2n-1}(\cos \theta)}{\rho^{2n+1}} \\ & + \sum_{n=1}^{\infty} \sum_{m=1}^{\infty} M_{2n-1} \frac{2(-1)^{n+1}}{\pi(2n-1)!} \frac{(-1)^{m+1}}{(2m-1)!} (2m-1) \rho^{2m-2} P_{2m-1}(\cos \theta) \int_0^{\infty} t^{2n-1} \frac{K_1(t)}{I_1(t)} t^{2m-1} dt \end{aligned}$$

and apply the boundary condition (3.2)

$$\begin{aligned} \frac{\partial}{\partial \rho} \phi(\lambda, \theta) = & -V \cos \theta = -V P_1(\cos \theta) = \sum_{n=1}^{\infty} M_{2n-1} \frac{-2nP_{2n-1}(\cos \theta)}{\lambda^{2n+1}} \\ & + \sum_{n=1}^{\infty} \sum_{m=1}^{\infty} M_{2n-1} \frac{2(-1)^{n+1}}{\pi(2n-1)!} \frac{(-1)^{m+1}}{(2m-1)!} (2m-1) \lambda^{2m-2} P_{2m-1}(\cos \theta) \int_0^{\infty} t^{2n-1} \frac{K_1(t)}{I_1(t)} t^{2m-1} dt. \end{aligned}$$

We now must swap m and n in the last sum

$$-VP_1(\cos\theta) = \sum_{n=1}^{\infty} M_{2n-1} \frac{-2nP_{2n-1}(\cos\theta)}{\lambda^{2n+1}} + \sum_{n=1}^{\infty} \sum_{m=1}^{\infty} M_{2m-1} \frac{2(-1)^{m+1}}{\pi(2m-1)!} \frac{(-1)^{n+1}}{(2n-1)!} (2n-1)\lambda^{2n-2} P_{2n-1}(\cos\theta) \int_0^{\infty} t^{2m-1} \frac{K_1(t)}{I_1(t)} t^{2n-1} dt.$$

Therefore,

$$-VP_1(\cos\theta) = \sum_{n=1}^{\infty} \left[M_{2n-1} \frac{-2n}{\lambda^{2n+1}} + \sum_{m=1}^{\infty} M_{2m-1} \frac{2(-1)^{m+1}}{\pi(2m-1)!} \frac{(-1)^{n+1}}{(2n-1)!} (2n-1)\lambda^{2n-2} \int_0^{\infty} t^{2m-1} \frac{K_1(t)}{I_1(t)} t^{2n-1} dt \right] P_{2n-1}(\cos\theta).$$

Substituting

$$M_{2n-1} = V \frac{A_n \lambda^{2n+1}}{2n}, \quad (3.8)$$

we obtain

$$P_1(\cos\theta) = \sum_{n=1}^{\infty} \left[A_n + \sum_{m=1}^{\infty} \lambda^{2n+2m-1} A_m \frac{2(-1)^{m+n+1}}{\pi(2m)!(2n-2)!} \int_0^{\infty} t^{2(m+n-1)} \frac{K_1(t)}{I_1(t)} dt \right] P_{2n-1}(\cos\theta). \quad (3.9)$$

We define coefficients B_{mn} as [19]

$$B_{mn} = \frac{2(-1)^{n+m+1}}{\pi(2m)!(2n-2)!} \int_0^{\infty} t^{2(n+m-1)} \frac{K_1(t)}{I_1(t)} dt. \quad (3.10)$$

Substituting B_{mn} into (3.9),

$$P_1(\cos\theta) = \sum_{n=1}^{\infty} \left(A_n + \sum_{m=1}^{\infty} \lambda^{2n+2m-1} A_m B_{mn} \right) P_{2n-1}(\cos\theta).$$

By equating coefficients,

$$A_n + \sum_{m=1}^{\infty} \lambda^{2n+2m-1} A_m B_{mn} = \begin{cases} 1 & \text{if } 1 = 2n - 1 \\ 0 & \text{if } 1 \neq 2n - 1 \end{cases}. \quad (3.11)$$

Using the Kronecker delta function

$$\delta_{ij} = \begin{cases} 1 & \text{if } i = j \\ 0 & \text{if } i \neq j \end{cases},$$

we can write (3.11) as

$$A_n + \sum_{m=1}^{\infty} \lambda^{2n+2m-1} A_m B_{mn} = \delta_{1n}. \quad (3.12)$$

The convergence of this system of equations is proved in [2]. We start to solve this system of equations by assuming that each coefficient is a series in λ

$$A_n(\lambda) = \sum_{s=0}^{\infty} K_{ns} \lambda^s. \quad (3.13)$$

Substituting (3.13) into (3.12),

$$\sum_{p=0}^{\infty} K_{np} \lambda^p + \sum_{m=1}^{\infty} \lambda^{2n+2m-1} \sum_{s=0}^{\infty} K_{ms} \lambda^s B_{mn} = \delta_{1n}.$$

After rearranging,

$$\sum_{p=0}^{\infty} K_{np} \lambda^p + \sum_{m=1}^{\infty} \sum_{s=0}^{\infty} B_{mn} K_{ms} \lambda^{2n+2m+s-1} = \delta_{1n}.$$

We wish to equate the coefficients of λ to its various powers. To accomplish this, we

define

$$p \equiv 2n + 2m + s - 1.$$

Thus,

$$\sum_{p=0}^{\infty} K_{np} \lambda^p + \sum_{m=1}^{\infty} \sum_{p=2n+2m-1}^{\infty} B_{mn} K_{m(p+1-2n-2m)} \lambda^p = \delta_{1n}. \quad (3.14)$$

Figure 3.2 illustrates how the double-summation is reversed to

$$\sum_{p=0}^{\infty} K_{np} \lambda^p + \sum_{p=2n+1}^{\infty} \sum_{m=1}^{\frac{p+1-2n}{2}} B_{mn} K_{m(p+1-2n-2m)} \lambda^p = \delta_{1n}. \quad (3.15)$$

We now examine this equation for various values of p with the intention of equating the coefficients of λ to its various powers. For $p = 0$,

$$K_{n0} \lambda^0 = \delta_{1n}.$$

For $0 < p < 2n + 1$,

$$K_{np} \lambda^p + 0 \lambda^p = \delta_{1n}.$$

For $2n + 1 \leq p$,

$$K_{np} \lambda^p + \sum_{m=1}^{\frac{p+1-2n}{2}} B_{mn} K_{m(p+1-2n-2m)} \lambda^p = \delta_{1n}.$$

We now equate the coefficients of λ to its various powers to obtain the recurrence relation:

$$\begin{aligned} K_{n0} &= \delta_{1n} && \text{for } 1 \leq n, \\ K_{np} &= 0 && \text{for } 1 \leq n, \ 0 < p < 2n + 1, \\ K_{np} + \sum_{s=1}^{\frac{p+1-2n}{2}} B_{sn} K_{s(p+1-2(n+s))} &= 0 && \text{for } 1 \leq n, \ 2n + 1 \leq p. \end{aligned}$$

The dependencies in this recurrence relation are illustrated in Figure 3.3.

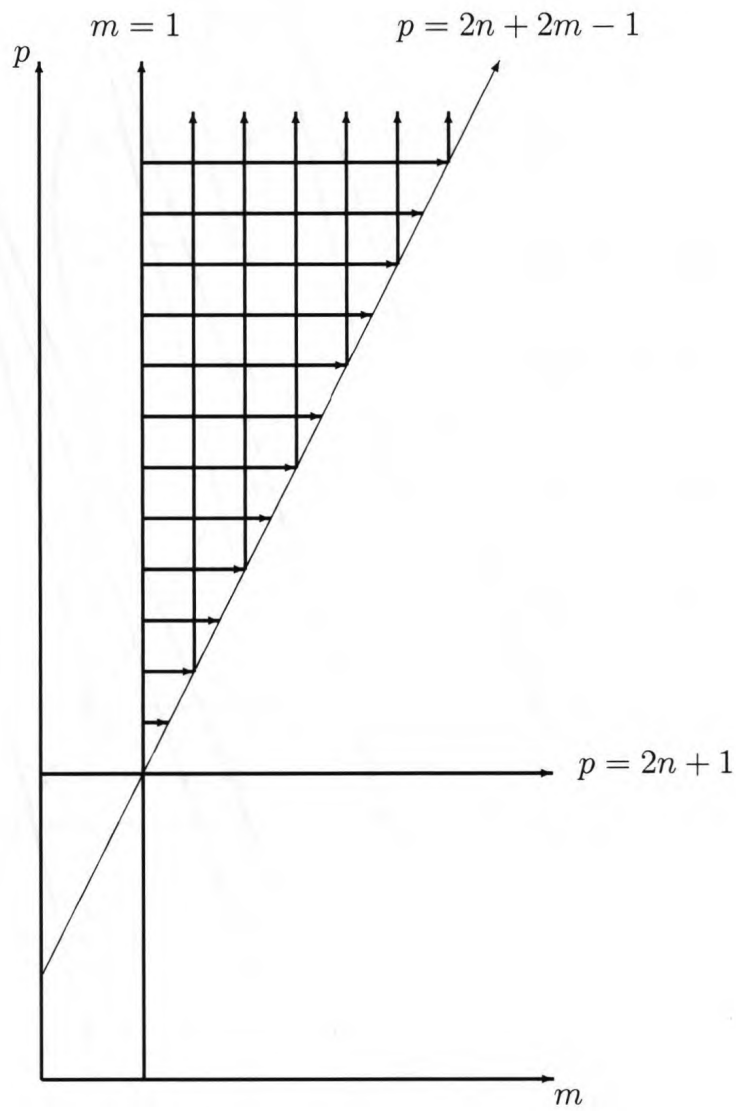


Figure 3.2: The domain for the double-summation $\sum_{m=1}^{\infty} \sum_{p=2n+2m-1}^{\infty} \dots$ in (3.14).
 The double-summation is reversed to $\sum_{p=2n+1}^{\infty} \sum_{m=1}^{\frac{p+1-2n}{2}}$ in (3.15).

K_{np} Coefficient Dependencies

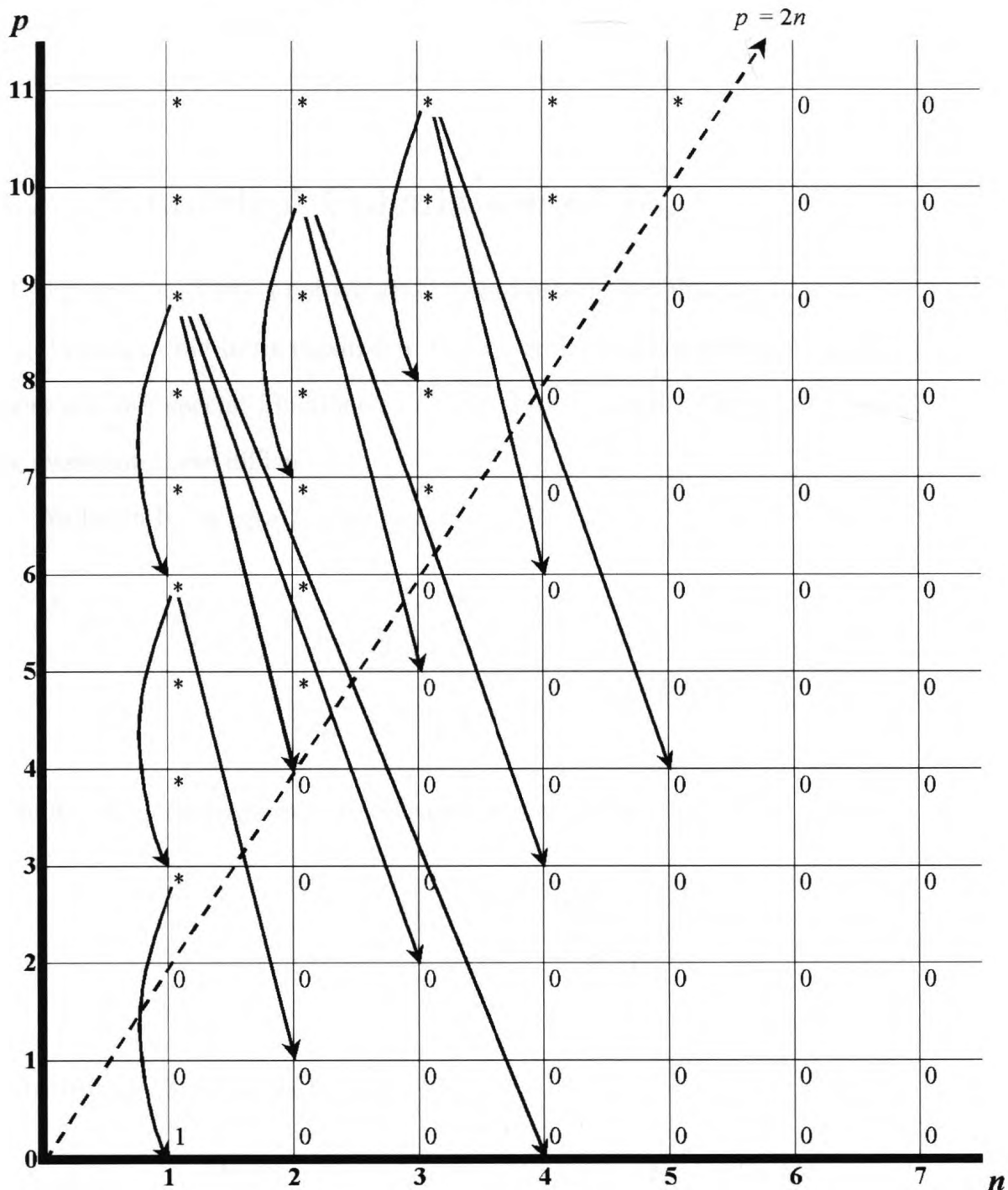


Figure 3.3: The dependencies for many of the K_{np} coefficients. The dashed line follows the equation $p = 2n$. All of the coefficients that are on or below this line are 0 except for k_{10} which is 1. Above the dashed line, all of the coefficients have potentially non-zero values that are dependent on other K_{np} coefficients. The solid-lined arrows indicate these dependencies for some of the coefficients. For example, $K_{(2)(10)}$ is dependent on K_{27} , K_{35} , and K_{43} . The dependencies for many of the coefficients are omitted to make the figure less cluttered.

This type of solution works well if the quantity of interest is some single item. For example if we want only the effective increase in resistance then we need only A_1 and it is a single series with computable coefficients.

3.2 Numerical Calculation of B_{mn}

The integral in (3.10) is not convenient for numerical evaluation because the function $K_1(t)$ contains $\ln t$ in its expansion, the integrand reaches extremely high values, and there are two special functions that must be evaluated. This section describes how we overcome these difficulties.

We begin by integrating by parts:

$$\int_0^\infty t^{2m+2n-2} \frac{K_1(t)}{I_1(t)} = \left[\frac{K_1(t)}{I_1(t)} \frac{t^{2m+2n-1}}{2m+2n-1} \right]_0^\infty - \frac{1}{2m+2n-1} \int_0^\infty t^{2m+2n-1} \frac{K_1'(t)I_1(t) - K_1(t)I_1'(t)}{I_1^2(t)} dt. \quad (3.16)$$

The following derivatives were obtained using Maple:

$$I_1'(t) = I_0(t) - \frac{I_0(t)}{t},$$

$$K_1'(t) = -K_0(t) - \frac{K_1(t)}{t}.$$

Substituting these derivatives into (3.16),

$$\int_0^\infty t^{2m+2n-2} \frac{K_1(t)}{I_1(t)} = \frac{1}{2m+2n-1} \int_0^\infty t^{2m+2n-1} \frac{K_0(t)I_1(t) + K_1(t)I_0(t)}{I_1^2(t)} dt.$$

Using the identity [20],

$$\frac{K_0(t)I_1(t) + K_1(t)I_0(t)}{I_1^2(t)} = -\frac{1}{tI_1^2(t)},$$

we find an alternative expression for B_{mn} :

$$B_{mn} = \frac{2(-1)^{n+m+1}}{\pi(2m)!(2n-2)!(2n+2m-1)} \int_0^\infty \frac{t^{2(n+m-1)}}{I_1^2(t)} dt.$$

This expression is more convenient to numerically evaluate than our original expression for B_{mn} . However, its integrand still reaches extremely high values. This problem can be rectified by utilizing the asymptotic expansion

$$\frac{1}{I_1^2(t)} \sim \frac{\pi}{(e^t)^2} \left(2t + \frac{3}{2} + \frac{21}{16t} \right) + \mathcal{O}\left(\frac{1}{t^2}\right)$$

This expansion was obtained using Maple. In order to reduce the maximum magnitude of the integrand, we can subtract any number of these expansion terms from it. In order to compensate for this subtraction, we can algebraically evaluate the integral of the expansion terms that were subtracted and add this result outside of the integral.

The simplest example is to utilize only the first term of the asymptotic expansion. For simplicity, we substitute $j \equiv m+n$. In order to utilize the first term, we must algebraically evaluate $\int_0^\infty \frac{2\pi t^{2j-1}}{e^{2t}} dt$. We start by integrating by parts:

$$\int_0^\infty \frac{t^{2j-1}}{e^{2t}} dt = \left[-\frac{t^{2j-1}}{2e^{2t}} \right]_0^\infty + \frac{2j-1}{2} \int_0^\infty \frac{t^{2j-2}}{e^{2t}} dt \quad (3.17)$$

$$= \frac{2j-1}{2} \int_0^\infty \frac{t^{2j-2}}{e^{2t}} dt. \quad (3.18)$$

We make the following definition:

$$\Upsilon_\kappa = \int_0^\infty \frac{t^\kappa}{e^{2t}} dt$$

Now, (3.18) can be written as

$$\Upsilon_{2j-1} = \left(\frac{2j-1}{2}\right) \Upsilon_{2j-2}.$$

Performing successive expansions,

$$\begin{aligned} \Upsilon_{2j-1} &= \left(\frac{2j-1}{2}\right) \Upsilon_{2j-2} \\ &= \left(\frac{2j-1}{2}\right) \left(\frac{2j-2}{2}\right) \Upsilon_{2j-3} \\ &= \dots \\ &= \left(\frac{2j-1}{2}\right) \left(\frac{2j-2}{2}\right) \dots \left(\frac{2}{2}\right) \left(\frac{1}{2}\right) \Upsilon_0 \\ &= \left(\frac{2j-1}{2}\right) \left(\frac{2j-2}{2}\right) \dots \left(\frac{2}{2}\right) \left(\frac{1}{2}\right) \int_0^\infty \frac{1}{e^{2t}} dt \\ &= \left(\frac{2j-1}{2}\right) \left(\frac{2j-2}{2}\right) \dots \left(\frac{2}{2}\right) \left(\frac{1}{2}\right) \left(\frac{1}{2}\right) \\ &= \frac{(2j-1)!}{2^{2j}}. \end{aligned}$$

Thus,

$$\int_0^\infty \frac{2\pi t^{2j-1}}{e^{2t}} dt = \frac{\pi(2j-1)!}{2^{2j-1}}$$

and

$$\int_0^\infty \frac{t^{2(j-1)}}{I_1^2(t)} dt = \frac{\pi(2j-1)!}{2^{2j-1}} + \int_0^\infty t^{2(j-1)} \left[\frac{1}{I_1^2(t)} - \frac{2\pi t}{e^{2t}} \right] dt.$$

To further improve the numerical efficiency, more of the asymptotic expansion terms can be subtracted from the integrand in the same manner. Figure 3.4, Figure 3.5, Figure 3.6, and Figure 3.7 illustrate how this technique significantly decreases the maximum value of the integrand.

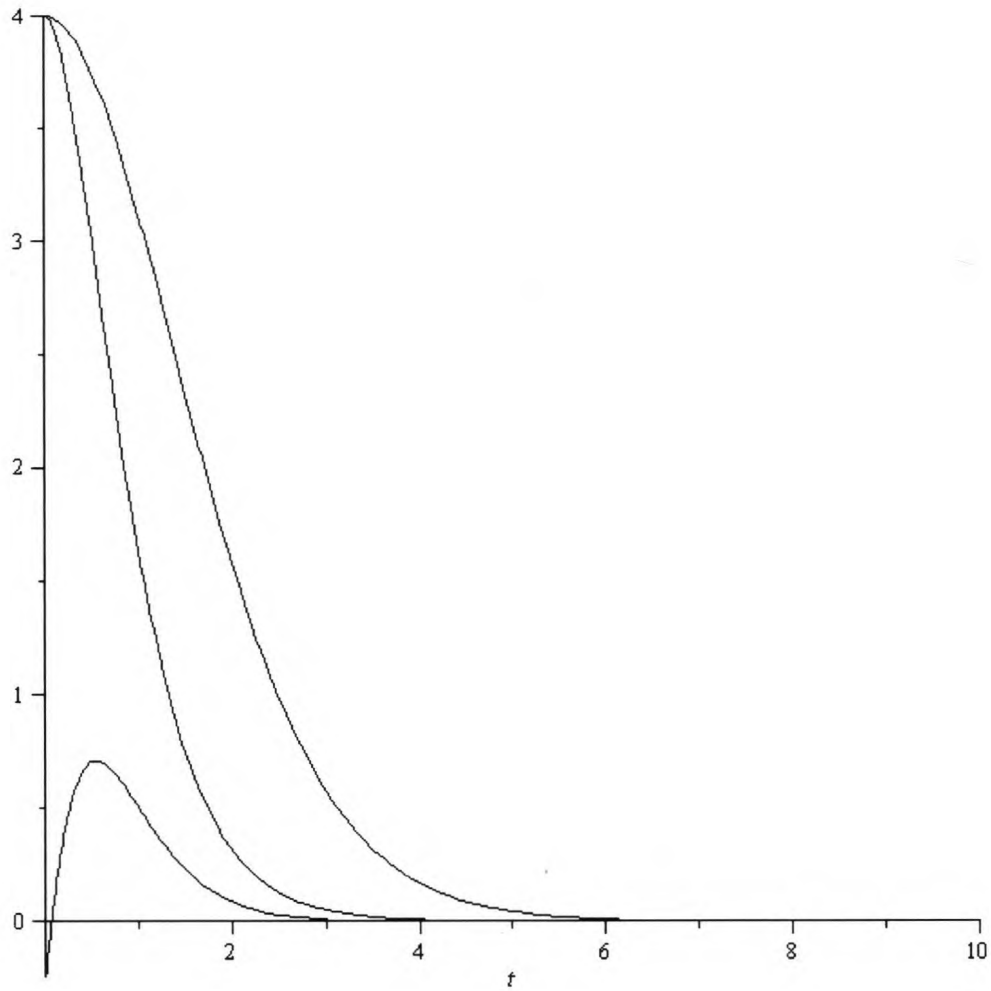


Figure 3.4: Graph showing three different integrands with respect to t . The top plot is the original integrand $\frac{t^{2(j-1)}}{I_1^2(t)}$ with $j = 2$. The middle plot is the original integrand with the first and second asymptotic expansion terms subtracted. The bottom plot is the original integrand with the first, second, third, and fourth asymptotic expansion terms subtracted.

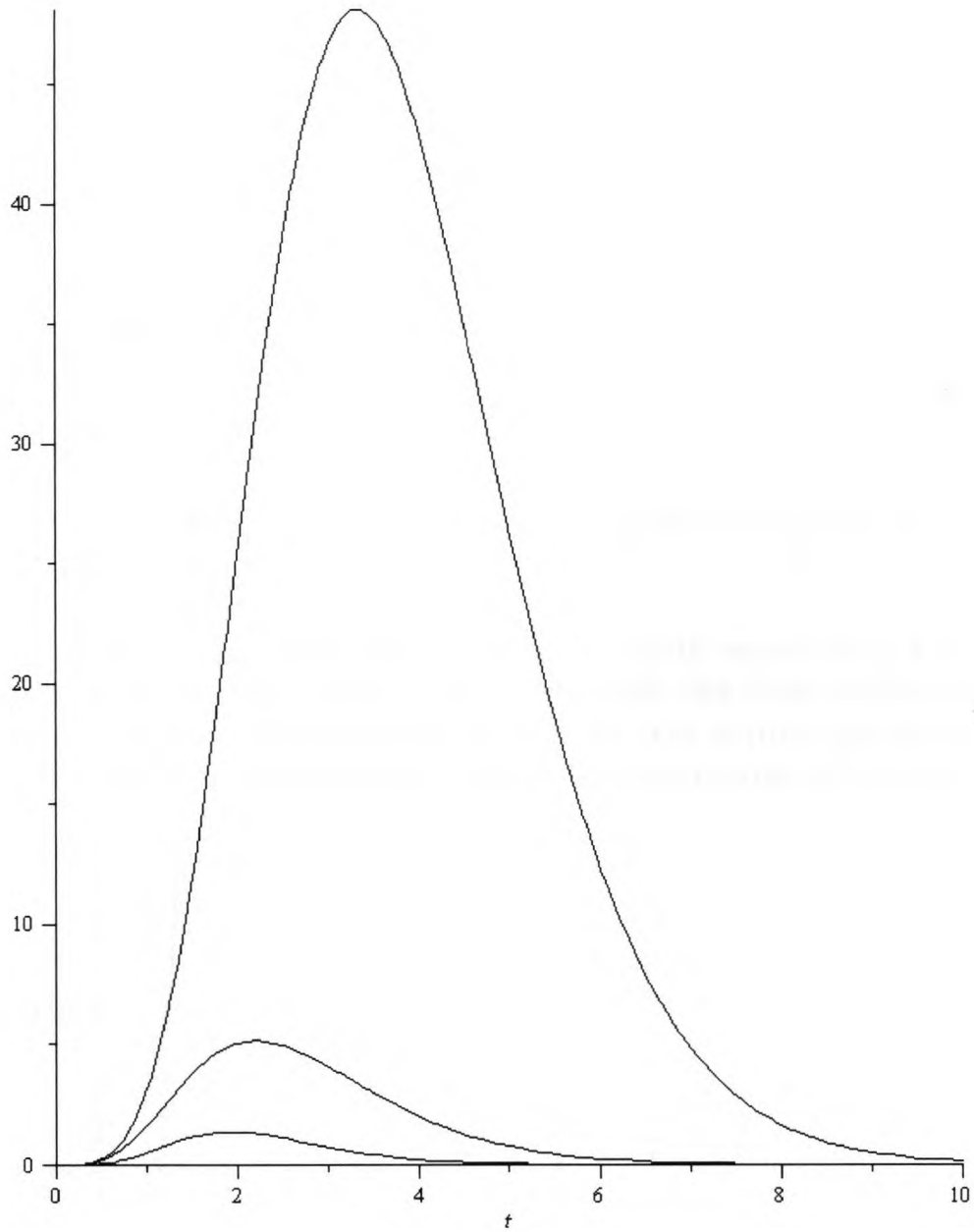


Figure 3.5: Graph showing three different integrands with respect to t . The top plot is the original integrand $\frac{t^{2(j-1)}}{I_1^2(t)}$ with $j = 4$. The middle plot is the original integrand with the first and second asymptotic expansion terms subtracted. The bottom plot is the original integrand with the first, second, third, and fourth asymptotic expansion terms subtracted.

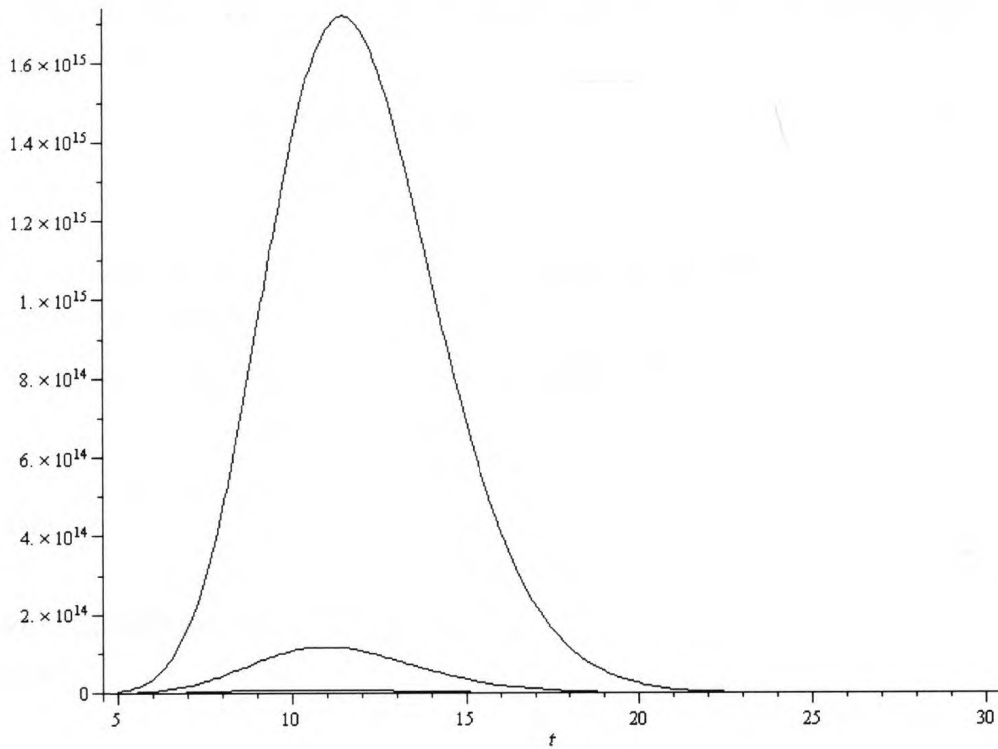


Figure 3.6: Graph showing three different integrands with respect to t . The top plot is the original integrand $\frac{t^{2(j-1)}}{T_1^2(t)}$ with $j = 12$. The middle plot is the original integrand with the first asymptotic expansion term subtracted. The bottom plot is the original integrand with the first and second asymptotic expansion terms subtracted.

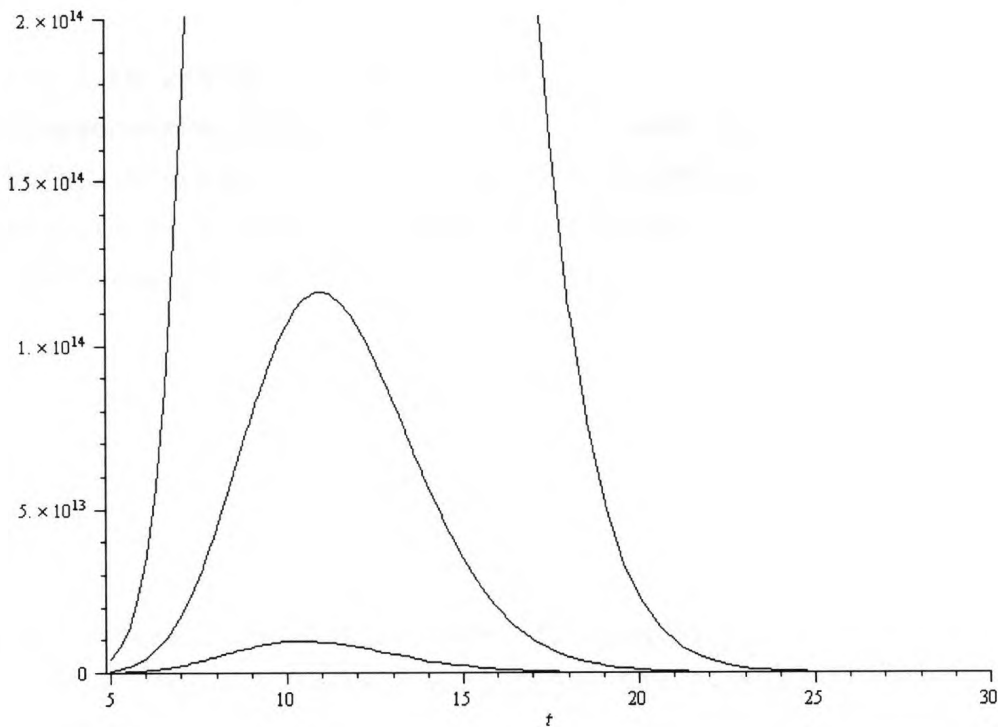


Figure 3.7: A zoomed in view of the bottom portion of Figure 3.6.

3.3 Numerical Calculation of K_{np} Coefficients

The following Maple code was used to calculate the K_{np} coefficients that are described in (3.13):

```
# The following procedure returns the matrix of the
# lambda coefficients.
#  $A[i] = \sum_{j=0}^{\infty} K[i,j] \lambda^j$ 

gc():
st := time():

ChangeoverParameter:=30;
Digits:=15;
P:=100;
N:=floor((P+1)/2)-1;

K:=Array(1..N,0..P):
BessInt:=Array(1.. 2*N):
B:=Array(1 .. N, 1 .. N):

for j from 2 to 2*N do      ## j = m+n
  if j>ChangeoverParameter then Digits:=9; end if;
  BessInt[j] := evalf( Pi * ((2*j-1)! / 2^(2*j-1) )
    +evalf(Int( t^(2*j-2)*(BesselI(1,t)^(-2)
      - 2*Pi*t*exp(-2*t)),t=0..infinity));
end do;

Digits := 15:

for m from 1 to N do
  for n from 1 to N do
    B[m,n] := evalf(BessInt[m+n]*2*(-1)^(m+n+1)
      /(Pi*factorial(2*m)*factorial(2*n-2)*(2*m+2*n-1)));
  end do;
end do;
```

```

for n from 1 to N do
  for p from 0 to P do
    K[n,p] := 0;
  end do;
end do;

K[1,0] := 1;

for p from 3 to P do
  for n from 1 to floor((p-1)/2) do
    x := 0;
    for s from 1 to floor((p+1-2*n)/2) do
      x := x + K[s,p+1-2*(s+n)]*B[s,n];
    end do;
    K[n,p] := -x;
  end do;
end do;
#unassign('x'): unassign('y'): unassign('n'):

time() - st;
K[1][P];

Kplot := [seq([ n,evalf(K[1,n]*2*sqrt(2)
  /( Pi*(-1)^n*binomial(-1/2,n)))] , n=0..P)]:
plot(Kplot, v=0..P, style=point,symbol=circle,color=[black]);

L2 := [seq([ n,evalf( ( K[1,n] - Pi*(-1)^n*binomial(-1/2,n)
  / (2*sqrt(2)))/((-1)^n*binomial(1/2,n)))] , n=1..P)]:
plot(L2, w=0..P, style=point,symbol=circle,color=[black]);

```

This code includes a constant known as the *ChangeoverParameter*. This constant can be varied to sacrifice accuracy in order to achieve a faster computation time. Table 3.1 shows the computed value of $K_{(1)(81)}$ and the computation time for various values of *ChangeoverParameter*.

<i>ChangeoverParameter</i>	Computed Value	Computation Time (seconds)
1	0.0683002478594672	468.674
5	0.0683002476982358	429.829
10	0.0683002477488312	463.760
20	0.0683002477481718	497.908
30	0.0683002477481718	402.014
40	0.0683002477481718	438.362
50	0.0683002477481718	391.453
60	0.0683002477481718	454.025

Table 3.1: The computed value of $K_{(1)(81)}$ and the computation time for various values of *ChangeoverParameter*. The computation time appears to be erratic because the method of measurement is not sufficiently accurate.

Theoretically, the computation time should increase as *ChangeoverParameter* is increased. However, the tabulated results do not indicate this as the computation time appears to be erratic. This is because the increase in computation time is greatly outweighed by the inaccuracy of our method for measuring the computation time. This Maple code was executed on a personal computer and many uncontrollable factors such as background tasks caused the erratic measurements.

3.4 Expression for Potential Drop

The effect of introducing a spherical obstacle is an increase in the difference of the potential between the two ends of the cylinder. According to (3.4), this increase is 2η , which has not yet been calculated.

To calculate this value, we use (3.7). In this equation, for terms with $1 < n$, as z approaches infinity, these terms approach 0. Thus, the only term that we will consider is the term with $n = 1$. This term is

$$\phi_1(r, z) = M_1 \int_0^\infty \frac{2}{\pi} t \left[\frac{K_1(t)}{I_1(t)} I_0(tr) + K_0(tr) \right] \sin(tz) dt.$$

Though this integral does not converge, the theory of generalized functions can be

used to show that, as $z \rightarrow \infty$, [12]

$$\int_0^\infty \frac{2}{\pi} t \left[\frac{K_1(t)}{I_1(t)} I_0(tr) + K_0(tr) \right] \sin(tz) dt \rightarrow 2 \operatorname{sgn} z.$$

Therefore, as $z \rightarrow \infty$,

$$\phi(r, z) \rightarrow M_1 2 \operatorname{sgn} z.$$

Using (3.8), we conclude that, as $z \rightarrow \infty$,

$$\phi(r, z) \rightarrow V A_1 \lambda^3 \operatorname{sgn} z.$$

Using (3.4),

$$\eta = V A_1 \lambda^3$$

and the increase in the difference of the potential between the two ends of the cylinder is

$$\Delta\phi = 2\eta = 2\lambda^3 V A_1.$$

3.5 Asymptotic Behaviour

After we obtain the series expansion for the solution, we should consider the speed of convergence of the series and the efficiency for computing the numerical data. Many papers and textbooks from the 19th century (and even the 20th century) would present solutions to physics or engineering problems and end their discussion as soon as they had obtained a series expression for the solution. Since these expansions were typically obtained as perturbations around some simple state, they were most accurate for the least interesting cases. The series expansion that we have obtained also has this characteristic. It is an expansion around the state of no sphere being present and is most accurate for small spheres which only slightly perturb the field.

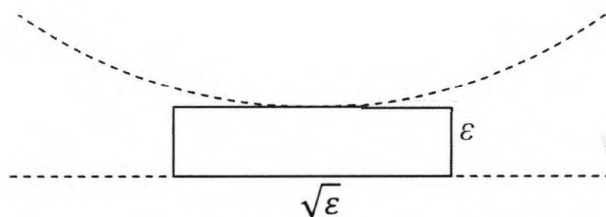


Figure 3.8: The geometry that used to obtain the asymptotic approximation. It is supposed that the gap between the sphere and the cylinder is ϵ and the extent of the gap in the z direction is $\sqrt{\epsilon}$.

As the sphere increases in size, it requires more and more terms, or equivalently, it becomes less and less accurate.

We should examine the asymptotic behaviour of the problem when the diameter of the sphere is almost the same as the diameter of the cylinder. The non-dimensional parameter $\epsilon = 1 - \lambda$ measures the gap between the sphere and the cylinder. This parameter is assumed to be much smaller than 1.

To accomplish this, we use a geometry that is described in [17]. In this case, two spheres had a small gap between them. This gap was approximated as a rectangle with a width of ϵ and a length of $\sqrt{\epsilon}$. Note that this length is longer than the width because $\epsilon < 1$. The justification for this approximation was based on approximating the sphere surface in the gap with a parabola. It was argued that, for a parabola $y = x^2$, the y coordinate increased by ϵ as the x coordinate increases by $\sqrt{\epsilon}$.

Applying this idea, we suppose that the gap between the sphere and the cylinder is ϵ and the extent of the gap in the z direction is $\sqrt{\epsilon}$. This geometry is illustrated in Figure 3.8. All of the electric field entering the wire must squeeze into this gap. Analogously, one could envision fluid flow squeezing into the gap. Inside the gap, the field is magnified by $\frac{1}{\epsilon}$ and the length of the gap is $\sqrt{\epsilon}$. Therefore, the potential drop must be of order $\frac{1}{\sqrt{\epsilon}}$.

The most interesting part of this analysis is that it can be tested using the series solution obtained above. More extensive analysis predicts the constant of proportion-

ality and we can write

$$A_1 = \frac{\pi}{2\sqrt{2}}(1 - \lambda)^{-\frac{1}{2}} + \mathcal{O}((1 - \lambda)^{\frac{1}{2}}).$$

Thus, if we expand the asymptotic solution with respect to λ , we obtain the series

$$A_1 = \frac{\pi}{2\sqrt{2}} \sum_{p=1}^{\infty} (-1)^p \binom{-\frac{1}{2}}{p} \lambda^p + \mathcal{O}((1 - \lambda)^{\frac{1}{2}}).$$

The expression $\binom{-\frac{1}{2}}{p}$ is defined in Section 3.6. We also made the assumption for the general solution that the coefficient expands as (3.13). By matching the two forms of the solution we predict that, as $p \rightarrow \infty$,

$$K_{1p} \rightarrow \frac{\pi}{2\sqrt{2}} (-1)^p \binom{-\frac{1}{2}}{p}. \quad (3.19)$$

If this prediction is true, then as $p \rightarrow \infty$,

$$\frac{K_{1p}}{\frac{\pi}{2\sqrt{2}} (-1)^p \binom{-\frac{1}{2}}{p}} \rightarrow 1$$

To verify this prediction, we numerically evaluated this expression for increasing values of p . These values are plotted in Figure 3.9 and they strongly indicate the validity of this prediction.

Including the second term in the asymptotic expansion, we predict that, as $p \rightarrow \infty$,

$$K_{1p} \rightarrow \frac{\pi}{2\sqrt{2}} (-1)^p \binom{-\frac{1}{2}}{p} + \Omega (-1)^p \binom{\frac{1}{2}}{p}. \quad (3.20)$$

where Ω is an unknown constant. If so,

$$\frac{K_{1p} - \frac{\pi}{2\sqrt{2}} (-1)^p \binom{-\frac{1}{2}}{p}}{(-1)^p \binom{\frac{1}{2}}{p}} \rightarrow \Omega. \quad (3.21)$$

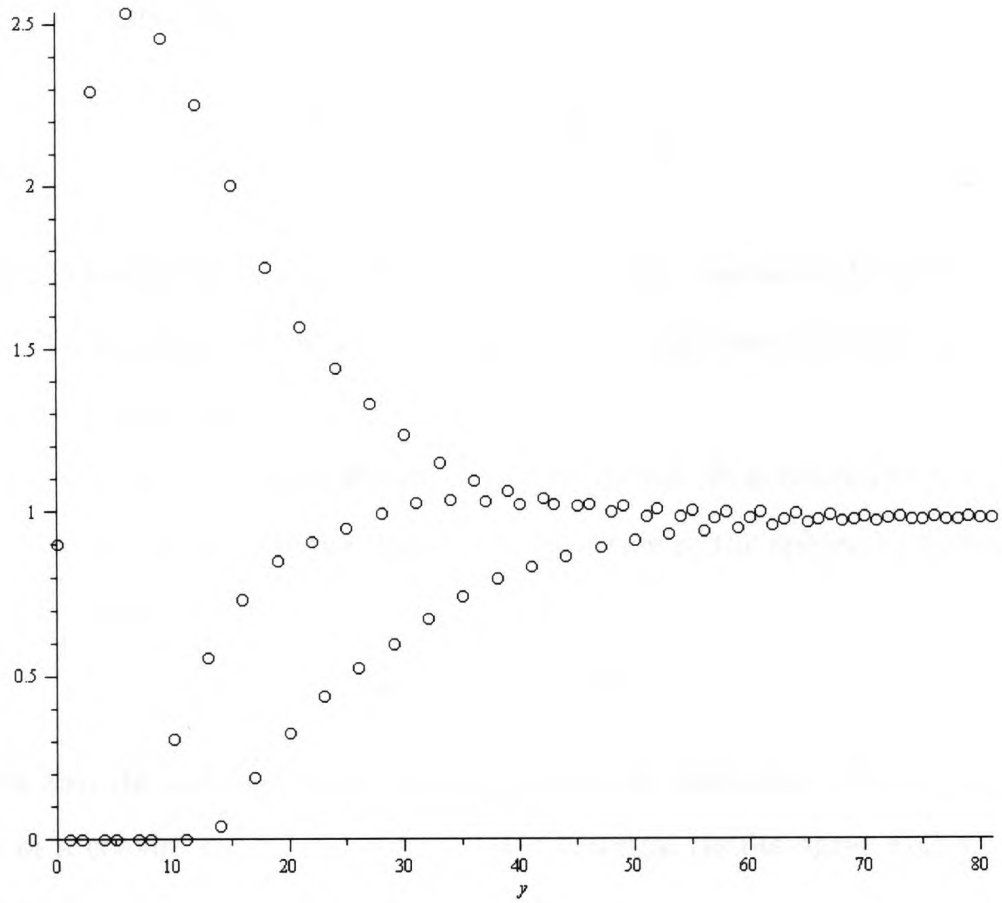


Figure 3.9: Graph of $\frac{K_{1p}}{\frac{\pi}{2\sqrt{2}}(-1)^p \binom{-\frac{1}{2}}{p}}$ versus p . This expression approaches 1 as p approaches infinity.

To verify this prediction, we numerically evaluated this expression for increasing values of p . These values are plotted in Figure 3.10 and they strongly indicate the validity of this prediction. Based on the numerical results, these values appear to converge at

$$\Omega = 2\sqrt{2}. \quad (3.22)$$

Therefore, we expect that, as $p \rightarrow \infty$,

$$\frac{K_{1p} - \frac{\pi}{2\sqrt{2}}(-1)^p \binom{-\frac{1}{2}}{p}}{2\sqrt{2}(-1)^p \binom{\frac{1}{2}}{p}} \rightarrow 1. \quad (3.23)$$

To verify this prediction, we numerically evaluated this expression for increasing values of p . These values are plotted in Figure 3.11 and they strongly indicate the validity of this prediction.

In applications, only the coefficient A_1 is of interest. It is related to the effective increase of length of the cylinder, due to the insertion of the sphere by formula (d is considered unitary)

$$\Delta L = \frac{\Delta\phi}{V} = 2\lambda^3 A_1.$$

This gives also the increase in resistance of the solid conducting cylinder due to the presence of a coaxial spherical bubble. The numerical results agree well with those obtained by Smythe [16], as indicated by Table 3.2.

3.6 Expansion of $\binom{-\frac{1}{2}}{p}$

In the previous section, (3.19) contained the expression $\binom{-\frac{1}{2}}{p}$. This is a non-typical application of the choose function because the first parameter is not a positive integer. This section explains the meaning of this expression in more detail. Since the first parameter is not a positive integer, we must use an alternative definition for the

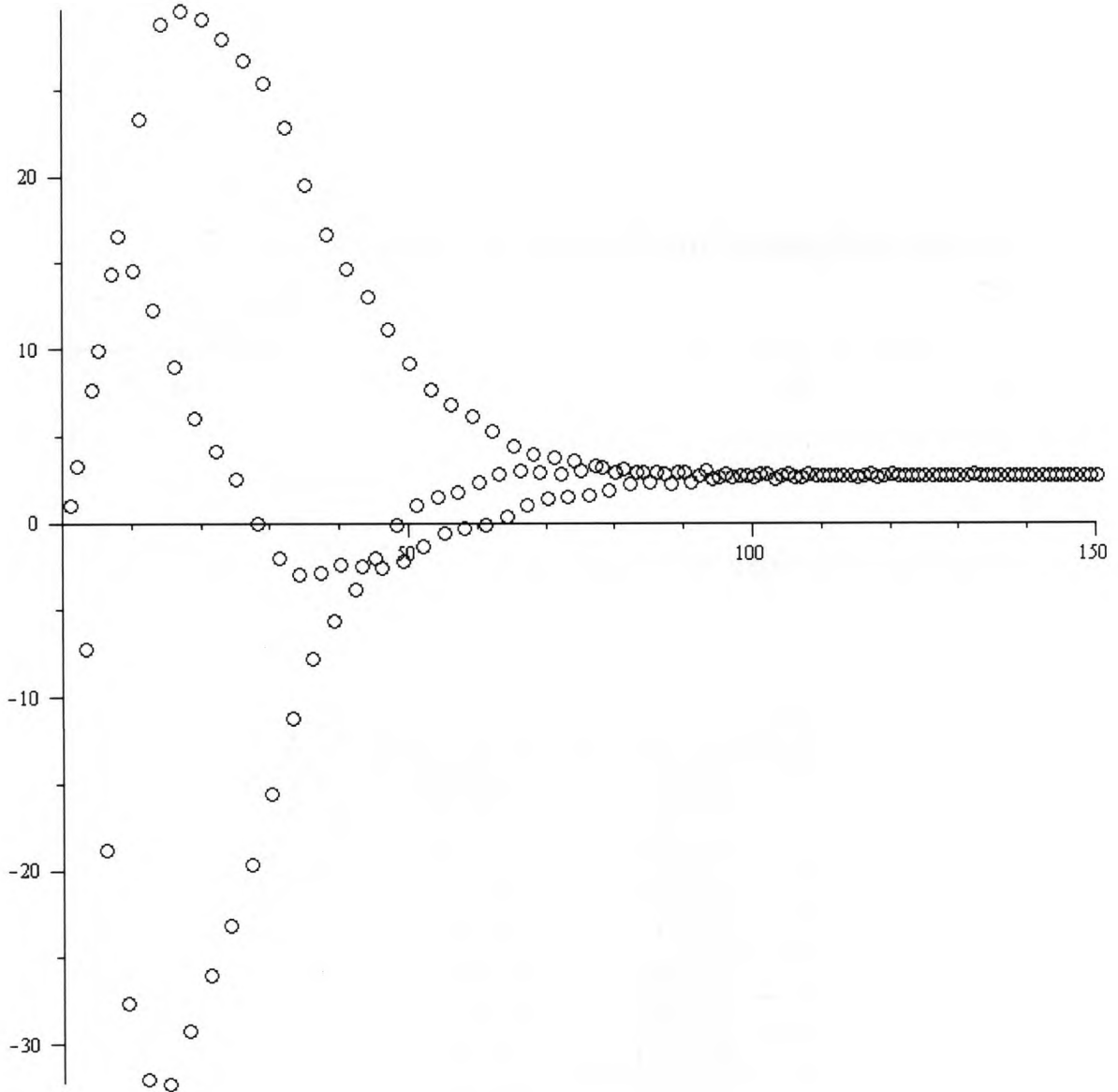


Figure 3.10: Graph of $\frac{K_{1p} - \frac{\pi}{2\sqrt{2}}(-1)^p \binom{-\frac{1}{2}}{p}}{(-1)^p \binom{\frac{1}{2}}{p}}$ versus p . This expression approaches a constant value as p approaches infinity.

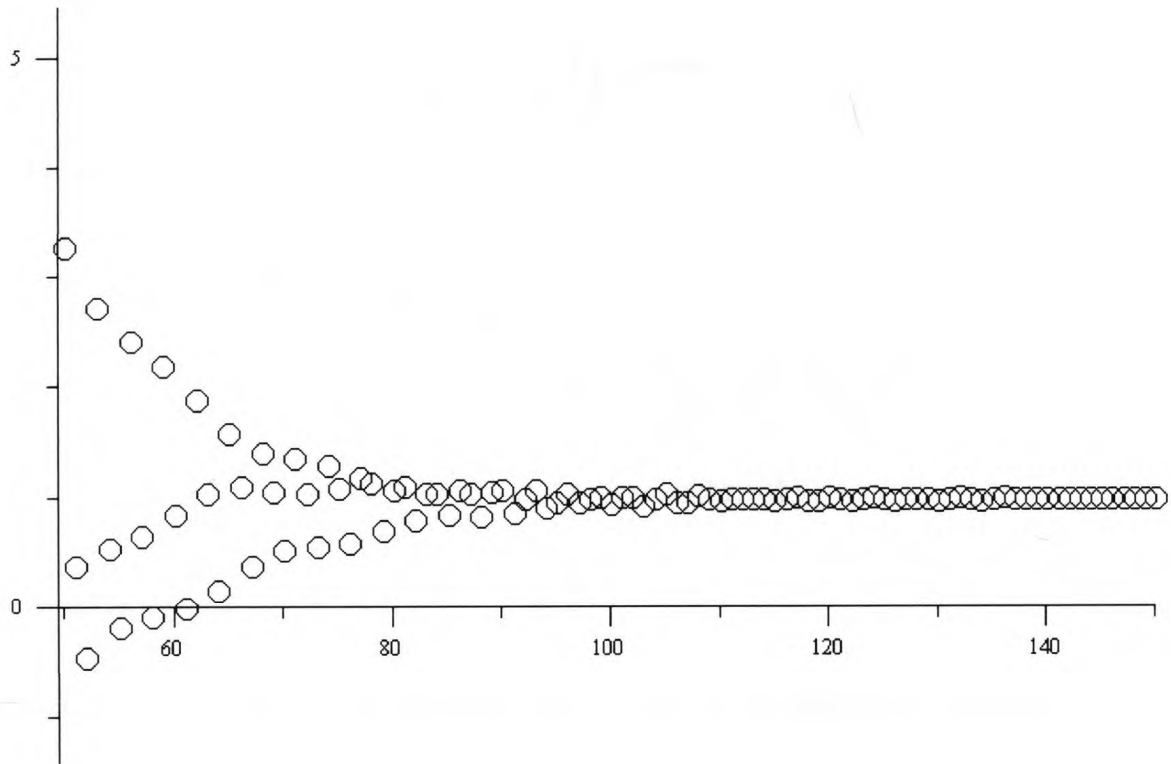


Figure 3.11: Graph of $\frac{K_{1p} - \frac{\pi}{2\sqrt{2}}(-1)^p \left(\frac{-1}{p}\right)}{2\sqrt{2}(-1)^p \left(\frac{1}{p}\right)}$ versus p . This expression approaches 1 as p approaches infinity.

λ	our results	Smythe's results
0.1	.0020015	.002002
0.2	.0161026	.016107
0.3	.0551873	.055187
0.4	.1348792	.134879
0.5	.2776735	.27767
0.6	.5220452	.52205
0.7	.9463394	.94634
0.8	1.751238	1.75124
0.9	3.727701	3.7277
0.95	6.620650	6.6207
0.96	7.794011	-
0.97	9.511413	-
0.98	12.34329	-
0.99	17.97598	-

Table 3.2: The increase in resistance of a solid conducting cylinder due to the presence of a spherical bubble, or the effective increase in the length of the cylinder

choose function [21]:

$$\binom{r}{k} = \frac{1}{k!} \prod_{n=0}^{k-1} (r - n).$$

In this case,

$$\begin{aligned} \binom{-\frac{1}{2}}{p} &= \frac{1}{p!} \prod_{n=0}^{p-1} \left(-\frac{1}{2} - n\right) \\ &= \frac{1}{p!} \left(-\frac{1}{2}\right) \left(-\frac{3}{2}\right) \left(-\frac{5}{2}\right) \cdots \left(-\frac{2p-1}{2}\right) \\ &= \frac{1}{p!} \left(-\frac{1}{2}\right)^p (1)(3)(5) \cdots (2p-1) \\ &= \left(-\frac{1}{2}\right)^p \frac{(2p-1)!!}{p!} \end{aligned}$$

where $\Upsilon!!$ denotes the double factorial function which is recursively defined as [22]

$$\Upsilon!! = \begin{cases} 1 & \text{if } \Upsilon = 0 \text{ or } \Upsilon = 1 \\ \Upsilon(\Upsilon - 2)!! & \text{if } \Upsilon \geq 2 \end{cases}.$$

This expression can be expanded further to avoid using the double factorial function.

$$\begin{aligned} \binom{-\frac{1}{2}}{p} &= \left(-\frac{1}{2}\right)^p \frac{1}{p!} \frac{(2p-1)!}{(2p-2)!!} \\ &= \left(-\frac{1}{2}\right)^p \frac{1}{p!} \frac{(2p)(2p-1)!}{(2p)(2p-2)!!} \\ &= \left(-\frac{1}{2}\right)^p \frac{1}{p!} \frac{(2p)!}{(2p)!!} \\ &= \left(-\frac{1}{2}\right)^p \frac{1}{p!} \frac{(2p)!}{2^p p!} \\ &= (-1)^p \frac{(2p)!}{[(2^p)(p!)]^2}. \end{aligned}$$

3.7 Conclusions

We utilize a symbolic-numeric approach to obtain a solution for the Laplace equation in a cylinder that contains a sphere. This mathematical solution is applicable to a number of physical problems. It can be used to calculate the increase in resistance of a wire due to the insertion of a non-conducting sphere. It can also be used to calculate the effective increase in length of a pipe due to the insertion of a sphere. It can also be used to model heat flow through a cylindrical heat conductor with a spherical insulator interrupting the heat flow. Theoretically, this technique can be used to model any physical parameter that is governed by the Laplace equation and the boundary conditions (3.1), (3.2), and (3.3).

The new feature of this technique is that Smythe's numerical solution is replaced with a more symbolic one. The unknown coefficients are expressed as a series expansion in the ratio of the sphere radius to the cylinder radius. This technique offers the advantage that the ratio of diameters is present as a parameter in the solution and the solution is valid for all ratios.

Bibliography

- [1] H. Brenner and J. Happel. *Low Reynolds Number Hydrodynamics*. Prentice-Hall, 1965.
- [2] C. M. Linton. Multipole methods for boundary-value problems involving a sphere in a tube. *IMA Journal of Applied Mathematics*, 55:187–204, 1995.
- [3] D. Halliday, R. Resnick, and J. Walker. *Fundamentals of Physics*. John Wiley and Sons, Inc., New York, fifth edition edition, 1997.
- [4] R. A. Adams. *Calculus: A Complete Course*. Addison-Wesley, Don Mills, e4 edition, 1999.
- [5] J. A. Stratton. *Electromagnetic Theory*. McGraw-Hill Book Company, Inc., New York, 1941.
- [6] E. W. Weisstein. Legendre polynomial. <http://mathworld.wolfram.com/LegendrePolynomial.html>.
- [7] C. H. Edwards and D. E. Penney. *Differential Equations and Boundary Value Problems: Computing and Modelling*. Prentice Hall, Upper Saddle River, second edition edition, 2000.
- [8] E. W. Weisstein. Taylor series. <http://mathworld.wolfram.com/TaylorSeries.html>.

- [9] The method of images. <http://www.phys.ufl.edu/dorsey/phy6346-00/lectures/lect04.pdf>.
- [10] R. Fitzpatrick. Classical electromagnetism: An intermediate level course. <http://farside.ph.utexas.edu/teaching/em/lectures/node64.html>.
- [11] I. M. Ryzhik and I. S. Gradshteyn. *Table of Integrals, Series, and Products*. Academic Press, Inc., San Diego, corrected and enlarged edition, 1980.
- [12] S. Ilie and D. J. Jeffrey. A note on laplace's equation inside a cylinder. *Applied Mathematics Letters*, 18:55–59, 2005.
- [13] R. C. Knight. The potential of a sphere inside an infinite circular cylinder. *Quart. J. Maths.*, 7:126, 1936.
- [14] J. C. Cooke. On potential problems involving spheroids inside a cylinder. 42:305–316, 1962.
- [15] W. R. Smythe. Flow around a sphere in a circular tube. *Phys. Fluids*, 4:756–9, 1961.
- [16] W. R. Smythe. Flow around a spheroid in a circular tube. *Phys. Fluids*, 7:633–7, 1964.
- [17] D. J. Jeffrey. The temperature field or electric potential around two almost touching spheres. *J. Inst. Maths Applics*, 22:337–51, 1978.
- [18] A. Erdélyi. *Tables of Integral Transforms*. McGraw-Hill Book Company, Inc., 1954.
- [19] D. J. Jeffrey, S. Ilie, J. M. Gardiner, and S. W. Campbell. A symbolic-numeric approach to an electric field problem. *Symbolic-Numeric Computation*, pages 349–359, 2007.

- [20] M. Abramowitz and I. A. Stegun. *Handbook of Mathematical Functions*. Dover Publications, Inc., New York, 1965.
- [21] Binomial coefficient. <http://planetmath.org/encyclopedia/BinomialCoefficient.html>.
- [22] E. W. Weisstein. Double factorial. <http://mathworld.wolfram.com/DoubleFactorial.html>.